UNIVERSITY OF CALIFORNIA
RIVERSIDE

A Neurocognitive Mechanism for Precision of Visual Working Memory Representations

A Dissertation submitted in partial satisfaction
of the requirements for the degree of

Doctor of Philosophy

in

Psychology

by

Weizhen Xie

June 2018

Dissertation Committee:
Dr. Weiwei Zhang, Chairperson
Dr. Steven E. Clark
Dr. Michael Yassa

The Dissertation of Weizhen Xie is approved:

_____

_____

_____

Committee Chairperson

University of California, Riverside

Acknowledgment

For me, graduate school is a period of intense learning, not only in the scientific arena, but also on a personal level. I could not complete this dissertation research without tremendous support from family, mentors, and friends. I would like to express my sincerest gratitude to all the people who have helped me along the way.

To begin with, I would like to thank my committee chair, Dr. Weiwei Zhang, who has become my academic mentor since I was an undergraduate research assistant at UC Davis. To me, Dr. Zhang is an exceptional advisor who provides continuous support, great patience, and genius insights. From the countless numbers of things that I have learned from him, these following things have greatly shaped my ways of thinking. First, his pursuit of *strong inference* has profoundly changed my perspective on scientific endeavors. That is, although there are many good ways of pursuing science, certain systematic methods of thinking with a focus on testing competing hypotheses may produce much more rapid progress than others. Second, his emphasis on "*Less is more*" and "*Replications are the best statistics*," potentially influenced by Dr. Steven J. Luck, exemplifies how *elegance* and *rigorousness* can be two wings of scientific discovery. Third, his openness to ideas is signified by his constantly open office door, of which I may have taken too much advantage. His constructive criticism and enthusiastic inquiry have always been keeping me on the right track in my research toward independence.

I would also like to thank my committee members, Dr. Steven E. Clark and Dr. Michael Yassa, who have provided professional support, insightful comments, and constructive suggestions on my dissertation research. Specifically, I greatly appreciate

Dr. Clark's witty and discerning remarks on details of my proposed experiments, which have helped perfect some procedural and analytical aspects of the experiments. I am also very grateful for Dr. Yassa's expert suggestions and generous support on neuroimaging data collection and data analyses. It would be impossible to complete Experiment 2 and 3 of this dissertation research without great contributions from his team, including Ms. Elizabeth A. Murray, Ms. Jessica Noche, Dr. Stephanie Leal, Ms. Maria Montchal, Dr. Zachariah Reagh, and Ms. Rebecca Stevenson. Relatedly, I would also like to thank Dr. Nicholas J. Tustison from University of Virginia for helping me perform hippocampal subfield segmentation in Experiment 3 and 4 through a collaboration with Dr. Yassa. Along this line, I also want to thank Dr. Xiaoping Hu, Dr. Jason Langley, Dr. Xu Chen, and Ms. Chelsea Savina Evelyn from the Center for Advanced Neuroimaging at UC Riverside, Dr. Edward Ester from Florida Atlantic University, and Dr. Gopikrishna Deshpande from Auburn University to make the discovery in Experiment 4 possible.

I must also express great appreciation to other committee members, departmental staff, and the funding source supporting my research. Dr. George J. Andersen, Dr. Rachel Wu, and Dr. Elizabeth Davis have served on my qualifying exam and/or second-year research project committees. Their insightful inputs have contributed to some ideas in my dissertation. Ms. Faye Harmer and Ms. Renee Young have helped handle numerous logistics before and during my dissertation research. This dissertation research is generously supported by the *Dissertation Year Program Award* and *Graduate Researcher Award* from Graduate Division of UC Riverside, a pilot project grant from the Center for

Advanced Neuroimaging of UC Riverside, and a neuroimaging seed grant awarded to Dr. Zhang from the Office of Research and Development of UC Riverside.

A special thank you goes to Dr. Robert Rosenthal, who is a true Pygmalion to his students. Beyond taking Dr. Rosenthal's classes as a first-year graduate student, I had the fortune to serve as his teaching assistant for graduate-level statistical courses in three academic years out of my five-year graduate school training. I have learned enormously from Dr. Rosenthal beyond knowledge about statistical procedures. I have lost count of how many afternoons Dr. Rosenthal has sat down with me in his office answering my questions, guiding me through some collaborative projects, and telling me enlightening anecdotes about how great minds have moved the field forward. His philosophy of teaching and characters of stellar scholarship will continue inspiring me on my journey towards academic independence.

I would also like to extend my gratitude to my fellow graduate students. I am indebted to Marcus Cappiello, my lab-mate, who has provided thoughtful comments to polish the research idea and has devoted time and efforts for data collection in Experiment 2 and 3. In addition, I could not survive graduate school without tremendous support from my apartment-mate, Parisa Parsafar, who has often offered beers, laughter, and kindness to keep life delightful in graduate school. I also want to thank my workout buddy Michael Dooley, restaurant-hunting friends Qiping Zhu and Lisa Ying Li, as well as other fellow graduate students who have been so kind to me all these years, including Anondah Saide, Angelica Falkenstein, Daniel Harmon, Hyung-bum Park, Erica Baranski, and many others.

Last but not the least, I would like to thank my parents and sister who give me unconditional love through the whole time of my life. My family is always the source of my strength. Words cannot express how much I love them. I sadly lost both of my grandmas during graduate school, who I could now only meet through memories. This dissertation is thus dedicated to my parents, sister, and late grandmas, to whom I hope to bring joys, comforts, and happiness.

To my parents and sister

In memory of my beloved grandmas

ABSTRACT OF THE DISSERTATION

A Neurocognitive Mechanism for Precision of Visual Working Memory Representations

by

Weizhen Xie

Doctor of Philosophy, Graduate Program in Psychology
University of California, Riverside, June 2018
Dr. Weiwei Zhang, Chairperson

Human memories do not always *precisely* correspond to exceedingly rich contents in the external environment. This variability of internal representations, especially in working memory (WM) – a system that maintains a small amount of information over a short time period at the service of other mental activities, sets an important functional limit in human cognition. However, neurocognitive mechanisms underlying this WM precision bottleneck remain unclear. One class of theories attributes WM precision to noisy sustained neural activity that supports WM retention (i.e., neural noise hypothesis). Another class of theories maintains that WM retention and precision are supported by independent neural mechanisms. Specifically, WM precision and its manifestation as a certain level of noise in sustained neural activity may be supported by pattern separation,

a computation potentially implemented in the hippocampus to orthogonalize similar memories into non-overlapping representations. This pattern separation hypothesis is preliminarily supported by 3 lines of evidence in 4 experiments of the current dissertation. First, in Experiment 1, observers with better pattern separation performance in a behavioral task tend to have higher precision in both WM and long-term memory (LTM), in contrast to a lack of significant association between pattern separation behavioral performance and the probability of successful remembering in either WM or LTM. Second, using functional Magnetic Resonance Imaging (fMRI), Experiment 2 shows that the hippocampus, along with several other regions in a distributed neural network, increases activity as the task demand on WM precision increases. This hippocampal sensitivity to WM precision task demand seems to be primarily driven by the DG/CA3 subfield – where pattern separation most likely occurs – in Experiment 3 using high-resolution fMRI. Third, Experiment 4 further demonstrates that the hippocampal DG/CA3, during WM delay period, retains decodable item-specific information, which further predicts activity in the visual cortices, potentially linking pattern separation to sensory recruitment for precise visual WM representations. Overall, these findings support a novel hippocampal pattern separation mechanism for WM precision, which is central to the ongoing debate on the nature of WM storage limitations. Articulating this potential mechanism may provide a better understanding of compromised mental clarity, manifested as reduced memory precision, in clinical populations such as schizophrenia and pathological aging, etc.

Table of Contents

List of Tables.....xiv

List of Figures.....xv

Chapter 1

Precision of Working Memory Representations: An Inquiry into Mental Clarity.....1

Working Memory and Its Roles in Cognition.....1

Quantitative and Qualitative Aspects of Memory Representations.....4

Quantity and Quality: Independent or Integrated Aspects of Working Memory?...7

Overview of the Current Dissertation.....11

Chapter 2

Neural Noise Hypothesis and Pattern Separation Hypothesis.....12

Neural Noise Hypothesis.....12

Pattern Separation Hypothesis.....14

Testing the Pattern Separation Hypothesis.....17

Chapter 3

Behavioral Association between Pattern Separation and Memory Precision.....19

Experiment 1: Correlations Between Behavioral Measures of Pattern Separation and Memory Precision.....20

Method.....20

Results and Discussion.....25

Conclusion.....26

Chapter 4

The Hippocampus is Sensitive to Task Demands on Working Memory Precision...27

Experiment 2: The Hippocampus Can Track Task Demands on Visual Working Memory Precision.....29

Method.....29

Results and Discussion.....36

Experiment 3: Working Memory Precision Related Neural Activity Across Hippocampal Subfields.....38

Method.....38

Results and Discussion.....41

General Discussion.....42

Conclusion.....45

Chapter 5

Decoding Precise Item-specific Working Memory Representation from Hippocampal DG/CA3.....46

Experiment 4: Decoding Working Memory Content in Hippocampal Subfields Using Inverted Encoding Model and High-resolution fMRI.....49

Method.....49

Results and Discussion.....57

Conclusion.....60

Chapter 6

General Discussion.....61

Summary of Findings.....61

Functional Roles of the Hippocampus in Human Cognition.....62

Precision and Capacity as Independent Aspects of Working Memory.....66

Translational Relevance.....68

Future Research Directions.....69

Appendix A Tables.....72

Appendix B Figures.....76

References.....89

List of Tables

Table 1. Brain areas activated monotonically to visual working memory precision load manipulation in Experiment 2.....73

Table 2. Results from psychophysiological interaction (PPI) analysis using the anterior and posterior hippocampi as separate seed regions in Experiment 2.....74

Table 3. Brain areas containing visual working memory content in Experiment 4.....75

List of Figures

Figure 1. Behavioral paradigms used in Experiment 1.....77

Figure 2. Associations among behavioral measures of pattern separation (i.e., lure discrimination index, LDI), mnemonic precision (SD), and the probability of successful remembering (Pm) across working memory and long-term memory in Experiment 1....78

Figure 3. Behavioral paradigm used in Experiment 2 and 3.....79

Figure 4. Recall error distributions and model fits across experimental conditions for data combining both inside scanner trials (100 trials per condition) and outside scanner trials (50 trials per condition) in Experiment 2 and Experiment 3.....80

Figure 5. Brain areas activated as a function of working memory precision load manipulation in Experiment 2.....81

Figure 6. Psychophysiological Interaction (PPI) results obtained by using the left anterior hippocampus (left aHPC, masked in yellow) and the left posterior hippocampus (left pHPC, masked in pink) as seed regions.....82

Figure 7. Activation in the DG/CA3 was monotonically modulated by precision load manipulation in Experiment 3.....83

Figure 8. Correlations between hippocampal activity and visual working memory probability of remembering, Pm (a) and precision, SD (b) in the high precision-load condition across Experiment 2 and 3.....84

Figure 9. Paradigm and the Inverted Encoding Model analysis in Experiment 4.....85

Figure 10. Behavioral and region-of-interest (ROI) results in Experiment 4.....86

Figure 11. Brain areas that contained decodable visual working memory content during the delay period in Experiment 4 based on a whole-brain searchlight analysis.....87

Figure 12. Granger causal relationship during the last 3TRs of the visual working memory delay period between hippocampal DG/CA3 and visual cortex ROIs extracted from the searchlight analysis.....88

Chapter 1

Precision of Working Memory Representations: An Inquiry into Mental Clarity

Memories are not always veridical representations of the past. How faithfully a given memory representation corresponds to a past event – *mnemonic precision* – may underlie *mental clarity* and its functional values in our everyday lives. For example, losses in mnemonic precision are often described as increases in "*brain fog*," such as the mind being "forgetful," "cloudy," and "lack of a focus" (Ocon, 2013; Ross, Medow, Rowe, & Stewart, 2013; Theoharides, 2015). These phenomenological experiences are frequently observed in compromised physical and mental health conditions, including coeliac disease (e.g., Yelland, 2017), chronic fatigue syndrome (e.g., Ocon, 2013), neuro-inflammation (e.g., Mackay, 2015; Theoharides, 2015; Theoharides, Stewart, Panagiotidou, & Melamed, 2016), fibromyalgia (e.g., Walitt et al., 2016), autism (e.g., Theoharides, Tsilioni, Patel, & Doyle, 2016), schizophrenia (e.g., Migliorati, Salvador, Adolescent, 2012, 2012), and aging (e.g., Maki & Henderson, 2016), etc. Although "brain fog" is an illustrative and easily-understood metaphor for reduced mental clarity (Parker et al., 2010), the mechanisms underlying these commonly-observed symptomatic complaints often vary across conditions and remain to be specified. To fill this gap in the literature, the current dissertation intends to examine a neurocognitive mechanism for precise mental representations retained in *working memory* (WM).

Working Memory and Its Roles in Cognition

WM, a concept popularized by Baddeley and Hitch (1974) to better capture short-

term memory (STM), is a system that supports temporary information retention (in the order of seconds) at the service of other ongoing mental activities (Atkinson & Shiffrin, 1968). Because STM representations are rarely maintained without prospective uses (Fuster, 2009), the term "working" is often preferred over "short-term" to describe processes and representations associated with *active* information maintenance (Baddeley, 2012). In comparison, long-term memory (LTM) is considered a system that primarily supports *passive* information storage for later uses in a more distant future (e.g., in hours or days after a memory event, Atkinson & Shiffrin, 1968). This distinction between WM and LTM in supporting different states/forms (active vs. passive) of memory representations has remained one of the primary research topics in cognitive psychology (Jonides et al., 2008).

Classical memory models consider WM as a unique cognitive system that is separate from the LTM system (e.g., the modal model, Atkinson & Shiffrin, 1968). As such, the neural mechanisms underlying active information maintenance and those underlying passive storage of memory representations may be independent of one another. This *system view* is supported by neuropsychological studies in brain-lesion patients. For example, patients with medial temporal lobe (MTL) lesions (e.g., H. M.) often exhibited anterograde amnesia with relatively intact WM task performance (Scoville & Milner, 1957); whereas, patients with prefrontal lobe lesions can manifest deficits in both WM (Voytek & Knight, 2010) and LTM (see a review in Simons & Spiers, 2003). However, an emerging *state view* of memory postulates that WM may be better conceptualized as activated LTM under the focus of attention (Cowan, 2001;

Oberauer, 2002). According to this view, WM as active LTM does not necessarily rely on different neural underpinnings as compared to passive LTM (Nee & Jonides, 2013a; 2013b). Supporting this conceptualization, recent human neuroimaging and neurophysiological recording studies have showed the involvement of MTL in some WM tasks (Hannula, Tranel, & Cohen, 2006; Libby, Hannula, & Ranganath, 2014; Kamiński, Sullivan, Chung, Ross, Mamelak, & Rutishauser, 2017). Furthermore, brain regions for LTM retrieval have also been shown to support maintenance of the same memory content in WM (e.g., Lewis-Peacock & Postle, 2008).

Notwithstanding these different theoretical viewpoints (system vs. state) on the architecture of human memory, WM (or active LTM) has several characteristics that are not necessarily shared by other cognitive processes. First, WM seems to be limited in storage capacity (G. A. Miller, 1956), such that only a small amount of information can be retained in WM (e.g., about 3 to 4 colors in visual WM, Cowan, 2001; Luck & Vogel, 1997; Zhang & Luck, 2008; but see Bays & Husain, 2008; Ma, Husain, & Bays, 2014; Oberauer & Lin, 2017). This limitation is in sharp contrast to a vast amount of information that can be stored in LTM (Brady, Konkle, Alvarez, & Oliva, 2008; Standing, 1973). Second, WM shows a complete loss of some retained information after a few seconds (Donkin, Nosofsky, Gold, & Shiffrin, 2015; Nosofsky & Donkin, 2016; Zhang & Luck, 2009). In comparison, LTM representations can be stored for days, months, or even years, and the primary reason for LTM forgetting may be interference instead of decay (Underwood, 1957). Third, WM – as a system integrating both bottom-up (stimuli-driven) and top-down (motivation and cognitive control) mental processes

(Baddeley, 2012; Cowan, 2001; Miyake & Shah, 1999) – has unique functional roles in cognition in that it supports a wide range of cognitive and affective functions. For example, larger WM storage capacity has been associated with more effective attentional allocation (Kane, Poole, Tuholski, & Engle, 2006), higher fluid intelligence (A. R. A. Conway, Kane, & Engle, 2003), more optimal processing of affective information (Lynn et al., 2016; Xie et al., 2017), and better emotional regulation (Schmeichel, Volokhov, & Demaree, 2008), etc.

Give the central role of WM in human cognition (Cowan, 2001), research articulating how precise mental representations can be actively retained in WM may thus reveal a key mechanism underlying mental clarity. This line of research may further provide translational insights to increased "brain fog" in some clinical conditions. Hence, the current dissertation will primarily focus on precision of mental representations in WM as a proxy toward a scientific inquiry into mental clarity. The following sections will introduce the operationalization of WM precision and discuss the nature of WM representations for later inquiries about potential mechanisms underlying WM precision in Chapter 2.

Quantitative and Qualitative Aspects of Memory Representations

When it comes to memory, both quantity and quality matter (Koriat & Goldsmith, 1996). The quantitative aspect of memory refers to the likelihood that a given stimulus is encoded into and retrieved from the mental *storehouse*, whereas the qualitative aspect of memory refers to the *correspondence* between internal mental representations and the corresponding external stimuli/events (Koriat & Goldsmith, 1994; 1996; Koriat,

Goldsmith, & Pansky, 2000). Although the qualitative aspect of mental representations, such as strength and vividness of memory, has been studied throughout the history of experimental psychology (Macmillan & Creelman, 2005), most empirical and theoretical research has emphasized the quantitative aspect of cognition (e.g., the number of items that one can remember in memory). Historically, this may be partly due to reductionism from the cognitive revolution (Bickle, 1998) and the movement away from Gibson's ecological approach (Koriat & Goldsmith, 1996). In memory research, this manifests as the declaration of the "*bankruptcy of everyday memory*" (Koriat & Goldsmith, 1996) and the popular *storehouse* approach (Koriat et al., 2000; Koriat & Goldsmith, 1996) that focuses on the quantitative aspect of internal representations and processes (e.g., Is a stimulus encoded into memory and properly retrieved?). However, the recently renewed interests in the qualitative aspect of memory (M. A. Conway, 1991; Gruneberg, Morris, & Sykes, 1991; Loftus, 1991) have profoundly shaped memory research in basic science (e.g., recognition memory, Parks & Yonelinas, 2007) and applied domains (e.g., eyewitness memory, Loftus, 2013).

For instance, recent studies have made substantial progress in developing models of these two aspects of memory representations to address theoretical and empirical questions (Bays & Husain, 2008; van den Berg, Awh, & Ma, 2014; Wilken & Ma, 2004; Zhang & Luck, 2008). One prominent model assesses the qualitative and quantitative aspects of memory based on their independent contributions to overall memory recall performance in a delayed estimation task (Zhang & Luck, 2008; 2009; 2011). In this task, observers memorize surface features of some briefly presented memory items, such as

colored squares, and then recall a given memory item after a delay of seconds (e.g., Zhang & Luck, 2008) or minutes (e.g., Brady, Konkle, Gill, Oliva, & Alvarez, 2013; Xie & Zhang, 2017b; 2018), by reproducing the remembered feature of the memory item on a continuous feature space, such as a circular color spectrum (Prinzmetal, Amiri, Allen, & Edwards, 1998; Wilken & Ma, 2004). According to the mixture model (Zhang & Luck, 2008; 2009; 2011), participants' recall performance across trials in this task reflects mixed contributions of both the quality and quantity of retained memory representations (Xie & Zhang, 2017a). Specifically, the qualitative aspect can be conceptualized as precision of retrieved memory, which is inversely related to the variability of recall performance based on retained memory. The quantitative aspect can be measured as the probability of successful memory retrieval, calculated as the probability of random responses subtracted from one.

Distinguishing these two aspects of memory using the mixture model is helpful to quantify different experimental effects on memory representations, such as memory impairments in clinical populations (e.g., J. M. Gold et al., 2010) and effects of sociobiological factors on memory, including sleep deprivation (e.g., Wee, Asplund, & Chee, 2013), emotion (e.g., Spachtholz, Kuhbandner, & Pekrun, 2014; Xie & Zhang, 2016; 2017b), and aging (e.g., Peich, Husain, & Bays, 2013), etc. Furthermore, this model can also clarify the dynamics of memory processes, such as encoding (Zhang & Luck, 2008) and forgetting (Zhang & Luck, 2009). For example, the gradual increase in the overall variability of memory performance in visual WM across retention intervals may be better accounted for by a decline in the likelihood of successful memory retrieval

(Donkin et al., 2015; Zhang & Luck, 2009) rather than by a decline in the quality of memory representations (Cornelissen & Greenlee, 2000; B. Lee & Harris, 1996; Paivio & Bleasdale, 1974).

Quantity and Quality: Independent or Integrated Aspects of Working Memory?

Using this mixture modeling approach, recent studies have further examined theoretically significant questions regarding the nature of WM limitations. That is, whether WM is constrained by a quantitative limit (i.e., capacity-limit, Zhang & Luck, 2008), a qualitative limit (i.e., precision-limit, Bays & Husain, 2008; van den Berg et al., 2014), or both (Alvarez & Cavanagh, 2004).

In this debate, capacity-limit theories attribute the storage limit in WM to capacity in that only a small number of discrete representations can be simultaneously retained in WM (Cowan, 2001; Luck & Vogel, 1997; Zhang & Luck, 2008). In contrast, precision-limit theories attribute the bottleneck of WM to the limit in the total amount of cognitive resource that can be flexibly divided among different WM representations (Bays & Husain, 2008). As the total pool of cognitive resource is finite, the amount of resource each representation receives would continuously decrease as the number of retained representations increases, leading to progressively reduced precision for each retained representation. As a by-product of this resource-sharing principle, observers could choose to remember either a small number of high-precision representations or a large number of low-precision representations (Bays & Husain, 2008; Ma et al., 2014), a tradeoff between the number and precision of retained memories. In contrast, capacity-limit theories suggest against this arbitrary tradeoff beyond WM storage capacity, such that the limit in

the number of items that an observer can retain in WM should be independent of the precision of those retained WM representations, even though more precise representations can be retained at the cost of reduced number of representations (but not vice versa). The core of this debate is thus whether the quantity (number) and quality (precision) of retained WM representations should be considered as *independent* or *integrated* aspects of WM.

Two distinctive approaches have been used in the literature to resolve this issue. First, a *behavioral dissociation approach* has been used to examine the independence between WM quantity and quality. According to this approach, if behavioral measures of these two aspects of WM are differentially associated with different experimental manipulations or individual differences, it is very likely that these two aspects of WM representations are supported by different (and likely to be independent) underlying mechanisms. For instance, interrupting the process of transferring fragile sensory information into WM (i.e., WM consolidation) using pattern masks at different time points following memory onsets can selectively affect the number, but not precision, of retained WM representations. In contrast, simultaneous white-noise masking of the memory array (e.g., random colors dots overlaying on top of to-be-remembered color squares) can reduce WM precision without reducing the number of retained WM items (Xie & Zhang, 2017a; Zhang & Luck, 2008). With a similar rationale, a growing literature has documented dissociable effects of individual differences in WM deficits due to certain health-related factors. For instance, sleep deprivation has been shown to compromise WM quantity instead of quality (Wee et al., 2013). In contrast, schizotypal

traits – as subclinical characteristics of schizophrenia spectrum disorders – has been associated with reduced WM quality instead of quantity (Xie et al., 2018). These empirical double dissociations between the quantitative and qualitative measures of WM thus provide important evidence for the independent nature of these two aspects.

However, critics of the behavioral dissociation approach argue that this approach is primary confirmatory in nature and often fail to consider all alternative models. Thus, the second approach uses formal *model comparison* and focuses on how well can competing models account for empirical data. For instance, to test competing hypotheses/theories, a recent study has tried to perform a factorial model comparison that assesses goodness-of-fit for models with different combination of assumptions (e.g., capacity-limit vs. capacity-unlimited, fixed precision across memory items vs. allowing precision to vary across memory items, van den Berg et al., 2014). Although there are great merits in this model comparison approach, a fundamental problem with this approach is that goodness of fit, while can serve as a good starting point for theory development, should not be the ultimate goal of cognitive science (Pitt & Myung, 2002; Roberts & Pashler, 2000; 2002; Rodgers & Rowe, 2002). As often observed in the literature, lots of competing models with fundamentally different conceptualizations of the underlying representations and processes can fit empirical data adequately well (Pitt & Myung, 2002). It is thus pivotal to establish the psychological meaning and validity of model parameters and to formulate testable predictions of a model (Roberts & Pashler, 2000; 2002) as advocated by the behavioral dissociation approach, which has unfortunately received little attention by the model comparison approach.

A similar theoretical dilemma can be found in the recognition memory literature, in which it is under heated debate whether recognition performance is supported by one process (i.e., memory strength, Wixted, 2007) or two different processes (Parks & Yonelinas, 2007; Yonelinas & Parks, 2007). The two competing theories, the *unitary-process* versus *dual-process* theories, again can account for various findings in the recognition memory literature adequately well, rendering the model comparison approach less informative (Yonelinas, Aly, Wang, & Koen, 2010). To move the field forward, cognitive neuroscience research using a *neural dissociation approach* has been proposed to evaluate the underlying cognitive and neural mechanisms supporting different aspects of a given model (Yonelinas et al., 2010). With this effort, recent neuropsychological and neuroimaging findings have shown that different aspects of recognition performance (e.g., remembering/knowing, source/item memory) may be differentially supported by the hippocampus and its surrounding structures (e.g., parahippocampus), mapping respectively to recollection and familiarity processes (Diana, Yonelinas, & Ranganath, 2007). As such, the dual-process theory that predicts dissociable cognitive and neural processes underlying recognition memory, as opposed to the unitary-process theory, may be able to better account for these observed neural patterns. Hence, demonstrating how different aspects of behaviors can be supported by different neural mechanisms may thus be informative in model selection (Yonelinas et al., 2010) beyond a mere focus on goodness-of-fit measures.

Similarly, if the quantitative and qualitative aspects of WM representations are supported by overlapping neurocognitive mechanisms, it is highly possible that the two

aspects are different manifestations of the same process. However, if the quantitative and qualitative aspects of WM are dissociable at the physical implementation level (Marr, 1982), it is possible that capacity and precision are independent constraining factors of WM representations. This neural dissociation approach is thus timely and critical for the current heated debate regarding the nature of WM representations. Furthermore, it may also provide a clue to a mechanism underlying mental clarity supported by precise WM.

Overview of the Current Dissertation

Going beyond behavioral dissociation and model comparison approaches, this dissertation will investigate a neurocognitive mechanism supporting WM precision, which may potentially be independent of the mechanism underlying WM capacity. Chapter 2 will elaborate this possible mechanism and an alternative hypothesis. Chapter 3 to 5 will describe studies designed to test predictions based on the proposed mechanism using different analytical or methodological approaches. Last, Chapter 6 will discuss some follow-up studies, translational significance, and future directions. Overall, by examining a plausible neurocognitive mechanism underlying WM precision, this dissertation research may provide better understandings for the nature of WM representations and for mental clarity that relies on precise WM.

Chapter 2

Neural Noise Hypothesis and Pattern Separation Hypothesis

Neural Noise Hypothesis

A recently developed *neural noise hypothesis* attributes WM precision to the variability of sustained neural activity underlying WM retention (Bays, 2014). Specifically, given that stimulus-selective persistent neural activity (Goldman-Rakic, 1995) or a propensity to produce persistent neural activity (Christophel, Klink, Spitzer, Roelfsema, & Haynes, 2017) has been considered as the neural correlate of WM retention, the variability of persistent neural activity is thus a natural candidate for the neural mechanism underlying the variability of retained WM presentations (Koyluoglu, Pertzov, Manohar, Husain, & Fiete, 2017; Veldsman, Mitchell, & Cusack, 2017), which is inversely related to WM precision. For example, persistent neuronal activity in the prefrontal cortex, which presumably underlie spatial WM performance, exhibits fluctuations during WM delay interval and produces systematic shifts in WM representations and variability in behaviors (Wimmer, Nykamp, Constantinidis, & Compte, 2014). Consequently, frontal and parietal mechanisms that reduce internal noise via attention modulation (see N. E. Myers, Stokes, & Nobre, 2017 for a review) or distraction inhibition (N. E. Myers, Stokes, Walther, & Nobre, 2014; Poliakov, Stokes, Woolrich, Mantini, & Astle, 2014) can increase WM precision. This neural noise hypothesis for WM precision can thus be naturally integrated into the mechanism for WM retention. That is, properties of the neural mechanisms for sustained neural activity

may give rise to both capacity and precision limits in WM. For instance, the upper limit in sustained activity during WM retention may be associated with WM capacity (Todd & Marois, 2004; Vogel & Machizawa, 2004), whereas the variability in sustained neural activity may account for WM precision (Bays, 2014; 2015). Another prediction of the neural noise hypothesis is that neural noise in multiple brain regions can be related to WM precision, given the distributed nature of WM retention in the brain (Eriksson, Vogel, Lansner, Bergström, & Nyberg, 2015; Veldsman et al., 2017). This integrated mechanism thus makes it straightforward to account for some previously observed relationships between WM quantity and quality, such as the dynamic tradeoff between the number and precision of retained WM representations (Banta Lavenex, Boujon, Ndarugendamwo, & Lavenex, 2015; M. A. Cohen, Konkle, Rhee, Nakayama, & Alvarez, 2014; Roggeman, Klingberg, Feenstra, Compte, & Almeida, 2014).

However, there are at least two concerns about the neural noise hypothesis. First, variability of sustained neural activity in the cerebral cortex can be the *consequence* or downstream effect of memory precision (i.e., neural manifestation of noisy memory representation), rather than the *cause*. For instance, decreased visual WM precision due to aging (Noack, Lövdén, & Lindenberger, 2012; Peich et al., 2013) may be a consequence of aging-related decline in the mid-brain dopaminergic function, which can manifested as an increased level of neural noise in the cortex (S.-C. Li, Lindenberger, & Sikström, 2001). Second, since WM retention is supported by a wide range of neural substrates (Courtney, Ungerleider, Keil, & Haxby, 1997; Eriksson et al., 2015; Mackey & Curtis, 2017; Veldsman et al., 2017), precision of WM representations can also be

affected by multiple factors, including precision of perceptual encoding (Emrich, Riggall, LaRocque, & Postle, 2013; Ester, Anderson, Serences, & Awh, 2013; FitzGerald, Moran, Friston, & Dolan, 2015; Pratte, Park, Rademaker, & Tong, 2017) and attentional control (see N. E. Myers et al., 2017 for a review) in parietal (Galeano Weber, Peters, Hahn, Bledowski, & Fiebach, 2016) and prefrontal (Sarma, Masse, Wang, & Freedman, 2015) regions. Although these factors are all important for maintaining precise WM representations, they may not be the *de facto* mechanism for WM precision. For instance, the significant decrease in precision of internal representations from perception to WM (Brady et al., 2013; Cappiello & Zhang, 2016; Chang, Armstrong, & Moore, 2012; Zhang & Luck, 2008) suggests potentially different mechanisms for WM precision and perceptual encoding. The latter can be significantly modulated by attentional mechanisms (Luck, Girelli, McDermott, & Ford, 1997; Palmer, 1990; Prinzmetal et al., 1998) such as gain control of neural activity in extrastriate visual cortices (Hillyard & Anllo-Vento, 1998), which can be independent of memory-related mechanisms.

Pattern Separation Hypothesis

In contrast to the integrated mechanisms for WM capacity and precision from the neural noise hypothesis, it is possible that the underlying mechanism for WM retention (e.g., neural oscillation, Raffone & Wolters, 2001) and that for WM precision are independent of each other, especially if the latter involves a universal computation to ensure efficient information processing. One plausible candidate for this universal computation is pattern separation, a process that orthogonalizes overlapping representations into more distinct forms (Marr, 1971). This computational process is

especially important for retaining precise memories in the presence of interference from highly similar distractors (Aimone, Deng, & Gage, 2011; Johnston, Shtrahman, Parylak, Gonçalves, & Gage, 2016), potentially including those in WM (Gilbert & Kesner, 2006). This memory resolving power seems to preferentially come from the hippocampus (Yassa & Stark, 2011), especially the Dentate Gyrus (DG). The three properties of the DG, including abundant granule cells, strong inhibitory interneurons, and powerful mossy fiber synapses, provide a highly efficient coding scheme to convert interference-susceptible population-coded information into interference-resistant sparse-coded representations (Aimone et al., 2011; Deng, Aimone, & Gage, 2010; Rolls, 2013; 2016). As a result of this pattern separation computation, precise individual representations can be retained in the hippocampus and later transferred to cortical regions to support accurate memory response (Marr, 1971). Consistent with this idea, some recent findings suggest that the hippocampus is important for remembering precise spatial and contextual information in LTM (Aimone et al., 2011; Johnston et al., 2016; Reagh & Yassa, 2014; Yassa & Stark, 2011). For instance, in the animal literature, lesions to the hippocampus, especially the DG, can impair mice's ability to recognize new spatial information that is similar to previously learned information (Clelland et al., 2009; Gilbert, Kesner, & Lee, 2001). Furthermore, human neuroimaging studies also demonstrate similar hippocampal sensitivity to pattern separation in object recognition memory tasks (e.g., Bakker, Kirwan, Miller, & Stark, 2008; Lacy, Yassa, Stark, Muftuler, & Stark, 2011; Reagh & Yassa, 2014).

However, this hippocampus-based mechanism for memory precision has been largely neglected by contemporary theories of WM, primarily due to the prominent system view of the dissociation between WM and LTM. According to the system view of memory, the MTL, especially the hippocampus, is exclusively involved in LTM but not in WM (Jeneson & Squire, 2012; Squire, 2017; Squire & Zola-Morgan, 1991). This system view is strongly supported by neuropsychological evidence showing that damages in the MTL (especially the hippocampus) often result in selective deficits in episodic LTM but not in WM (Baddeley & Warrington, 1970; Scoville & Milner, 1957; Sullvan & Sagar, 1991). It, however, has recently been challenged by some neuroimaging findings showing increased activities in MTL, including the hippocampus, in WM tasks (Axmacher et al., 2007; Barense, Gaffan, & Graham, 2007). Nonetheless, these findings could not rule out an alternative interpretation. Specifically, task performance in a WM task is often supported by various cognitive processes including WM. Consequently, hippocampal involvement in a WM task could reflect processes other than WM. For instance, MTL activities in WM tasks can be obtained when WM task load (e.g., set size or complexity) is high or when retention interval is relatively long (see Ranganath & Blumenfeld, 2005 for a review). As such, hippocampal involvement in a WM task with a large number of memory stimuli may thus result from LTM support for supra-capacity information (Jeneson & Squire, 2012; Jeneson, Mauldin, & Squire, 2010; Jeneson, Mauldin, Hopkins, & Squire, 2011; Jeneson, Wixted, Hopkins, & Squire, 2012). Similarly, hippocampal involvement in WM tasks for relational or complex information (Libby et al., 2014) could also simply be a result of increased capacity demand for

relational/complex information, instead of its specific involvement in WM. To address this alternative interpretation, it is pivotal to articulate the specific computational process that the hippocampus contributes to WM representations when LTM involvement is minimized (e.g., short delay period and low WM load).

Testing the Pattern Separation Hypothesis

The pattern separation hypothesis postulates that the hippocampus contributes to WM with its pattern separation computation to retain precise WM representations by de-correlating similar sensory inputs. This hypothesis and its three critical predictions will be tested in the present dissertation research.

Prediction #1: Increases in hippocampal pattern separation should be coupled with higher WM precision.

Prediction #2: The hippocampus, especially its DG/CA3subfield that has been implicated for pattern separation (Yassa & Stark, 2011), should be sensitive to different task demands on WM precision. That is, the hippocampus should be more involved when a WM task requires higher WM precision.

Prediction #3: The hippocampus should contain decodable WM content that reflects precise item-specific information retained during the delay period of a WM task.

Prediction# 1 can manifest as similar changes in pattern separation and WM precision due to certain experimental manipulations. For instance, induced negative emotion has been shown to improve both pattern separation (Segal, Stark, Kattan, Stark, & Yassa, 2012) and WM precision (Xie & Zhang, 2016). Alternatively, it could manifest as shared variance across the two constructs using an individual-differences approach.

That is, observers with better hippocampal pattern separation tend to show higher WM precision. To test this prediction, Experiment 1 in Chapter 3 thus uses a set of established behavioral paradigms to obtain measures about hippocampal pattern separation function and WM precision.

Moving beyond individual differences, *Prediction# 2* is tested using a combination of experimental and neuroimaging methods in Experiment 2 and 3 of Chapter 4. Specifically, Experiment 2 uses functional Magnetic Resonance Imaging (fMRI) methods in a visual WM task to identify brain regions, potentially including the hippocampus, that exhibit higher activity with increased task demands on WM precision. Experiment 3 will further pinpoint the hippocampal subfield(s) that potentially drive hippocampal contributions to WM precision using high-resolution fMRI.

Experiment 4 in Chapter 5 will test *Prediction #3* by using a novel decoding model and high-resolution fMRI. It is expected that precise item-specific information that is actively retained in WM can be decoded from the hippocampus, especially from the DG/CA3 subfield that has been implicated for pattern separation in human observers (Yassa & Stark, 2011).

These empirical tests of the three critical predictions from the pattern separation hypothesis will be summarized in Chapter 6. Additional predictions of the pattern separation hypothesis and potential follow-up experiments will also be discussed.

Chapter 3

Behavioral Association between Pattern Separation and Memory Precision

This chapter aims at establishing the behavioral association between pattern separation and mnemonic precision in visual memory. Pattern separation is often assessed using the mnemonic similarity task (S. M. Stark, Yassa, Lacy, & Stark, 2013). This task begins with an incidental study phase in which observers view a series of everyday objects and categorize these objects as "indoor" versus "outdoor" items. In a subsequent test phase, observers are presented with items that have been shown before (i.e., old), lures that are similar with but not identical to the old ones (i.e., similar), and foils that have never been presented in the previous study phase (i.e., new). Observers are asked to classify these items into corresponding categories (i.e., old, similar, or new) based on their memory. From these memory responses, pattern separation can be defined as a Lure Discrimination Index (LDI), which is the difference between the probability of reporting lure items as "similar" and the probability of reporting foil items as "similar." Using this paradigm, previous studies have shown that signals in the hippocampal DG/CA3 subfield could differentiate lures and old items (i.e., pattern separation), even when the similarity between lures and old items was high (Lacy et al., 2011). Furthermore, reduction in LDI has also been associated with compromised hippocampal functions in aging population (e.g., Yassa et al., 2010) and in hippocampus-damaged patients (e.g., Kirwan et al., 2012). Therefore, the LDI is often considered a behavioral measure for hippocampal pattern separation function (S. M. Stark et al., 2013).

Although hippocampal pattern separation has been hypothesized as the underlying computational process supporting mnemonic precision (Aimone et al., 2011; Severa, Parekh, James, & Aimone, 2017), the behavioral association between pattern separation and mnemonic precision has not been formally evaluated. To fill this gap in the literature, Experiment 1 correlates the behavioral measure of pattern separation, namely the LDI, and mnemonic precision of visual memory estimated from the recall paradigm for both WM and LTM. Previous studies have demonstrated that LTM also retains detailed feature information (Brady et al., 2008), which could be as precise as WM representations (Brady et al., 2013). According to the hippocampal pattern separation hypothesis, pattern separation serves as an underlying mechanism for mnemonic precision in both short-term and long-term memories. Consequently, it is expected that the LDI will be correlated with behavioral measures of mnemonic precision, but not with the quantitative aspect (i.e., probability of successful retrieval), of WM and LTM. In contrast, the neural noise hypothesis predicts no reliable relationship between pattern separation and mnemonic precision.

Experiment 1: Correlations Between Behavioral Measures of Pattern Separation and Memory Precision

Method

Participants. Sixty college students (19.58 ± 1.87 [Mean ± SD] years old, 22 males) participated in Experiment 1 for course credits at University of California, Riverside. All participants had normal color vision and normal (or corrected-to-normal) visual acuity. They provided written informed consent prior to the study.

Procedure. Each participant performed three tasks, namely the mnemonic similarity task (S. M. Stark et al., 2013), the WM color recall task (Zhang & Luck, 2008), and the LTM color recall task (Brady et al., 2013). The mnemonic similarity task was always run first. Two recall tasks followed the mnemonic similarity task with the order counterbalanced across participants. In all tasks, all stimuli were presented on a 60Hz LCD monitor (calibrated using an X-Rite I1Pro spectrophotometer) on a gray background (6.1 cd/m^2) at a viewing distance of 57 cm.

Mnemonic Similarity Task. An incidental study phase and a recognition test phase were presented in this task (Figure 1a). In the study phase, 128 images of everyday objects (2.9° to 12.9° of visual angle in width and 4.0° to 12.8° of visual angle in height) were sequentially presented in a random order at the center of the screen for 2,000 ms per image with a 500-ms inter-stimulus interval (S. M. Stark et al., 2013). Participants reported whether the image contained an indoor object or an outdoor object by pressing the "V" and "N" buttons on a standard keyboard, respectively. They were allowed up to 2,500 ms to make such a response following the presentation of the object. Participants were asked to respond as accurately as possible within the given time window. If the participant was unsure, they were instructed to make the best guess possible and to try to make a response to each image. In the subsequent test phase, 192 objects were sequentially presented in a random order at the center of the screen for 2,000 ms, each with a 500-ms inter-stimulus interval. One-third of the objects were exact repetitions of objects presented in the study phase (old items), one-third of the objects were new objects not previously seen (foils), and one-third of the objects were similar to those seen during

the study phase but not identical (lures). Participants categorized the presented test items into these corresponding categories, namely "old," "similar," and "new," by pressing the "V," "B," and "N" keys, respectively. Accuracy was stressed as long as participants responded within the appropriate time window (2,500 ms).

WM Color Recall Task. In this task (Figure 1b), participants were instructed to memorize a memory array with 5 color squares simultaneously presented on the screen for 400 ms. These colors were randomly chosen from 180 iso-luminant colors evenly distributed in the Commission Internationale de l'Eclairage Lab (CIELAB) color space (see Zhang, 2007 for details). Locations of the color squares were randomly selected from a set of eight possible locations that were equally spaced on an invisible circle (5.5° of visual angle in radius). After a short delay of 1,000 ms with a blank screen, an arrow cue was presented pointing to the location of a randomly selected memory item, along with a continuous color wheel with all 180 colors. Participants were required to report the color at the cued location using a computer mouse to click on the color wheel. Immediately afterwards, an arrow was drawn outside of the color wheel pointing to the correct color for 1000 ms as feedback. All participants completed 3 blocks of 50 trials, yielding 150 trials in total.

LTM Color Recall Task. One-hundred-and-twenty unique objects were randomly chosen from Brady et al.'s (2013) stimuli set which included 540 pictures of categorically distinct objects for the LTM task. These objects (6.5° × 6.5° of visual angle) could be recognized in arbitrary colors allowing their colors to be randomly rotated in hue space, yielding a different color appearance. The LTM color recall task also included a study

phase and a test phase. On each trial in the study phase, a random color value from 120 evenly distributed and iso-luminant color hues in a 360-degree CIELAB color space was assigned as the initial color of each object. These study objects were sequentially presented at the center of the screen for 2,000 ms with a 500-ms inter-stimulus-interval. Participants were explicitly told to remember the colors of the presented objects.

In a subsequent test phase (Figure 1c), participants saw an object from the study phase and tried to reconstruct its color on each trial. Each object was initially presented in gray scale. Participants rotated the mouse cursor, initially located at the center of the object, on an adjustment ring (7° of visual angle in diameter) centered on the test object, to continuously adjust the color of the object on a predefined invisible color wheel. The object's color was determined by the angular position of the mouse cursor (i.e., the angle of the line connecting the center of the test item and the location of the cursor). When the object was colored in a hue that participants believed to best match their memory, they clicked the left mouse button and the color value of the test item was recorded. Online feedback (1,000 ms) was provided as the difference between the color participants chose (indicated by a gray bar marking the angular position of the chosen color on the adjustment ring) and the actual color of the test object (indicated by a thicker black bar on the adjustment ring marking the angular position of the original color of the test object from the study phase). Participants proceeded at their own pace and were instructed to be as precise as possible to report the objects' colors. The order of objects in the test phase was independent of the order of objects in the study phase. There were two study-and-test blocks with 60 different objects per block, yielding a total of 120 recall trials.

Data Analysis. Participants' ability to perform pattern separation computation was assessed using the LDI, calculated as the difference between the probability of "similar" responses on the lure trials and the probability of "similar" responses on the foil trials (Kirwan et al., 2012). This score reflects how well can an observer tease part similar lures from old items (correctly identifying lures as "similar") after correcting for the general bias in "similar" responses (i.e., "similar" response to new items). Thus, a high LDI indicates better pattern separation ability.

Participants' performance in the recall tasks can be quantified by a recall error on each trial, calculated as the angular difference between the presented color in the memory array and an observer's reported color (ranged from -180° to 180°). The distributions of these recall errors across trials were fitted with Zhang and Luck's (2008) mixture model using Maximum Likelihood Estimation (MLE) procedure, separately for each subject at each condition. As previously introduced, in this model, the overall distribution of recall errors is conceptualized as a weighted summation of two components, namely a von Mises distribution representing graded and noisy memory representations for probed items that are encoded in memory and a uniform distribution for guessing responses when the probed items cannot be successfully retrieved from memory. The proportion/weight of the von Mises distribution represents the probability that the probed item is successfully retrieved (Pm). The width of the von Mises distribution, defined as the standard deviation (SD) of the von Mises distribution, is inversely related to mnemonic precision. That is, a smaller SD indicates higher memory quality. Overall, this mixture model accounted for more than 97% of the variance in the observed data

(adjusted R^2). Note, to keep consistent, both WM and LTM recall data were fitted with the same model. Critically, as formally tested in Richter et al. (2016) for LTM recall data, this mixture model (von Mises + uniform) substantially outperformed other competing models.

Results and Discussion

As summarized in Figure 2, Pearson correlations were calculated for the variables of interest (i.e., LDI, Pm_{LTM}, Pm_{WM}, SD_{LTM}, and SD_{WM}). Of primary interest, LDI was significantly correlated with the precision measures of both LTM (LDI and SD_{LTM}: r = -.38 [-.58, -.14], p = .0031) and WM (LDI and SD_{WM}: r = -.28 [-.50, -.03], p = .032). However, LDI was not significantly correlated with the probability of successful memory retrieval in LTM or WM (all *ps* > .60). Not surprisingly, the precision measures of LTM and WM from the two recall tasks were highly correlated with one another (SD_{LTM} and SD_{WM}: r = .37 [.13, .57], p = .0035). In contrast, probability of successful memory retrieval was not significantly correlated with each other (r = .10 [-.35, 16], p = .44). Critically, the correlation between LDI and SD_{WM} was significantly larger than the correlation between LDI and Pm_{WM} (Z = 1.84, p = .033, one-tailed), based on a one-tailed test on correlated correlations (Meng, Rosenthal, & Rubin, 1992). Similarly, the correlation between LDI and SD_{LTM} was also significantly stronger than the correlation between LDI and Pm_{LTM} (Z = 2.55, p = .0054, one-tailed). Furthermore, recognition accuracy of the new and old responses from the mnemonic similarity task was not significantly correlated with any measures of LTM or WM performance (Pm_{LTM}, Pm_{WM}, SD_{LTM}, and SD_{WM}; all *ps* > .20). These highly specific correlation patterns suggest that

the associations in task performance between the mnemonic similarity task (a recognition memory paradigm) and the recall tasks may be specifically driven by the qualitative aspects of memories, instead of by omnibus task performance such as accuracy.

Conclusion

Overall, this chapter demonstrates a considerate amount of shared variance in qualitative aspects of memory representations across visual LTM and WM (i.e., LDI, SD_{LTM}, and SD_{WM}). Furthermore, these measures of memory quality do not necessarily correlate with measures of memory quantity or compound measures of memory performance (i.e., Pm_{LTM}, Pm_{WM}, and recognition accuracy). These findings are consistent with the hypothesis that pattern separation computation underlies mnemonic precision across LTM and WM.

Chapter 4

The Hippocampus is Sensitive to Task Demands on Working Memory Precision

Building on the behavioral association between hippocampal pattern separation function and mnemonic precision, using fMRI, Chapter 4 aims to directly establish hippocampal involvement in visual WM precision by testing how the hippocampus responds to an experimental manipulation of task demands on WM precision. If the hippocampus contributes to WM precision, it is expected that hippocampal activity in a visual WM task will increase as the task demand on WM precision increases. In contrast, the neural noise hypothesis predicts comparable hippocampal activations under different task demands on WM precision, given that other brain regions beyond the hippocampus (e.g., frontal and parietal cortices) may support WM retention (Fuster & Alexander, 1971; Todd & Marois, 2004; Y. Xu & Chun, 2005; but see Kamiński et al., 2017).

Following this rationale, Experiment 2 and 3 directly manipulate the level of precision needed to correctly perform the color recall WM task by varying discriminability between memory and lure colors in a delayed estimation task (Zhang & Luck, 2011). Specifically, across different task demands on WM precision (Figure 3), to-be-remembered colors are randomly sampled from and later matched to either 1) 180 continuously varying colors used in Experiment 1 (precise memory for color shade is necessary for accurate recall, high-precision load condition), 2) 15 evenly distributed colors spokes from the 180 colors (less precise memory of color is sufficient for accurate recall, medium-precision load condition), or 3) 6 evenly distributed color spokes from the

180 colors (lower memory precision is enough to support accurate recall, low-precision load condition). A perceptual and motor control condition is also included, in which a color randomly sampled from the 180 colors is to be matched onto a simultaneously presented color wheel. In this control condition, while the memory component is minimized, the perceptual encoding and motor response components are comparable to the three memory conditions. To maximize the effectiveness of these manipulations, these different experimental conditions are blocked, with the order counterbalanced across participants using a Latin-squared design.

Considering that distributed brain regions are involved in WM (Eriksson et al., 2015), Experiment 2 adopts a whole-brain fMRI approach to identify a set of potential brain regions, including the hippocampus, that may be sensitive to task demands on WM precision. To further isolate the contributions of hippocampal subfields (especially DG/CA3) to visual WM precision, Experiment 3 uses a high-resolution fMRI sequence (Reagh, Murray, & Yassa, 2017) by focally scanning the temporal regions of the brain with a 1.8×1.8 mm^2 in-plate resolution in a 3-Tesla scanner. Considering the complicated folding structure of hippocampal subfields, larger voxel sizes from standard fMRI sequences (e.g., 3 mm^3) may contain signals from various subfields, making it difficult to isolate subfield-specific contributions to WM precision. The high-resolution fMRI approach (Carr, Rissman, & Wagner, 2010) is thus essential for the current testing hypothesis regarding the association between hippocampal DG/CA3, where pattern separation computation is most likely to occur (Yassa & Stark, 2011), and visual WM precision.

Experiment 2: The Hippocampus Can Track Task Demands on Visual Working Memory Precision

Method

Participants. Twenty right-handed participants (12 female, on average 23.07 ± 3.89 years old) were recruited from the Orange County community, Irvine, CA. All participants reported having normal color vision and normal (or corrected-to-normal) visual acuity. They also reported no history of neurological or psychiatric disorders and no history of psychostimulant use. The sample size of this study is predefined based on previous similar functional MRI studies (e.g., Reagh et al., 2017; Reagh & Yassa, 2014). All participants provided written informed consent following the procedure approved by the Institutional Review Board of both the University of California, Irvine and University of California, Riverside, and they received monetary compensation for their participation.

Behavioral Task. The behavioral paradigm was modified from the WM color recall task (Figure 3, also see Experiment 1 in Zhang & Luck, 2011). Each trial of the task started with a 2-second blank screen with a fixation point on the screen. Afterwards, 4 perceptually different color squares were briefly presented for 200 ms in 4 randomly selected locations from a set of 8 equally-spaced locations on an invisible circle (5.5° radius). This memory array was followed by an 1,800-ms delay interval with only a fixation circle on the screen. Immediately after this delay interval, a test array containing 4 placeholders at the original locations of the study colors was presented along with a color wheel. One of the placeholders was bolded. Participants were instructed to recall the color that was originally presented in the bolded placeholder (i.e., target color) based

on their memory, by using button presses to adjust the location of a cursor on the color wheel to land the cursor on the target color as precisely as possible. This cursor was initially presented at a random location on the wheel at the onset of the test display. By using the right index and middle fingers to press different buttons that mapped with the finger positions, participants moved the cursor clockwise and counterclockwise, respectively. They used the ring finger to press a third key to confirm their response. If participants did not confirm their response within the given response time window (3,750 ms), the last location of the cursor on the wheel was treated as their response. On average, participants' response time (onset of test display till the confirm response) was 2742 ms (std. = 441), which was within the response time window.

Three memory conditions were included to manipulate the load of WM precision. In the high encoding precision load condition, the study colors were randomly sampled from all 180 colors (with a minimum of 20° difference from one another) in the 360° color space (see Zhang & Luck, 2008 for details). In the medium encoding precision load condition, the study colors were randomly sampled from 15 fixed colors evenly distributed in the 360° color space (with a 24° difference for two adjacent colors). And in the low encoding precision load condition, the study colors were randomly sampled from 6 fixed colors that evenly distributed in the 360° color space (with a 60° difference for two adjacent colors). Note, in the low encoding precision load condition, the 6 fixed colors were chosen to be as close as possible to center around the self-report color categories in the set of 180 colors in an independent group of observers (see Zhang, 2007). In the test phase of these memory conditions, a corresponding color wheel was

presented matching the number of colors that was used to sample the study colors. A fourth perceptual/motor control condition was included, in which participants experienced similar trial events as those in the high encoding precision load condition. However, they had no need to remember items from the memory display, because in the later test display, the tested color would remain on the screen with the correct color marked on the color wheel at the onset of the test with a white arrow. Participants only needed to move the cursor to the target color through button presses.

Each block consisted of 50 trials of one of the four conditions. Participants were told at the beginning of each experimental block what condition they were in. There were 2 sequential blocks for each memory conditions and 1 block for the perceptual/motor control condition, in total 7 blocks/runs (350 trials). The order of different conditions was counterbalanced with a Latin-square design across participants. Before going into the scanner, participants completed additional 50 trials for each memory condition (across 6 blocks, 25 trial each) and additional 25 trials for the perceptual/motor control condition (1 block) for practice.

MRI Data Acquisition. Neuroimaging data were acquired on a 3.0 Tesla Philips Achieva scanner, using a 32-channel sensitivity encoding (SENSE) coil at the Neuroscience Imaging Center at the University of California, Irvine. A high-resolution 3D magnetization-prepared rapid gradient echo (MP-RAGE) structural scan (0.65 mm isotropic voxels) was acquired at the beginning of each session and used for co-registration. Functional MRI scans consisted of a T2*-weighted echo planar imaging (EPI) sequence using blood-oxygenation-level-dependent (BOLD) contrast: repetition

time (TR) = 2000 ms, echo time (TE) = 26 ms, flip angle = 70 degrees, 34 slices, 200 dynamics per run, 3 × 3 mm in-plane resolution, field of view (FOV) = 184 mm × 118 mm × 184 mm. Slices were acquired as a partial axial volume and without offset or angulation. A total of 7 functional runs were acquired for each participant, 6 for the memory conditions and 1 for the perceptual/motor control condition (order counterbalanced). Each functional run lasted 6 minutes and 40 seconds excluding 4 initial dummy scans acquired to ensure T1 signal stabilization.

Data Analysis for the Behavioral Task. As in Experiment 1, participants' behavioral performance on each trail in the continuous recall task was measured as the recall error capturing the angular difference between presented color in the memory array and reported color (ranged from -180° to 180°). Note, since the number of recall options was reduced in the medium encoding precision load and low encoding precision load conditions, participants' recall errors tended to cluster around a few bins even though they could choose freely on the wheel in between 2 color spokes. This introduced an artificial clustering nature of recall error distribution, making it difficult to reliably estimate the precision of retrieved memory representation especially in the low precision load condition (Zhang & Luck, 2011). That said, it was still possible to estimate the proportion of uniform distribution given that responses due to guessing would still evenly distributed across different bins. Thus, participants' recall error distributions under each experimental condition were divided into 12 bins and fitted with the mixture model separately for each subject at each condition based on binned data using simplex method (Lagarias, Reeds, Wright, & Wright, 1998).

Preprocessing of fMRI Data. All neuroimaging data were preprocessed and analyzed using the Analysis of Functional NeuroImages (AFNI, Cox, 1996) software on a Mac OSX platform, based on the standardized *afni_proc.py* pipeline. Specifically, despiked data (*3dDespike*) were corrected for motion (*3dvolreg*) and slice timing shifts (*3dTshift*), and masked to exclude voxels outside the brain (*3dautomask*). Functional scans were aligned to each subject's skull-stripped anatomical image (MP-RAGE) with *align_epi_anat.py*, and wrapped into the Montreal standard alas space (MNI-152) for later group analysis (*3dvolreg*, *3dAllineate*). These functional data were smoothed with a 6.0 mm Gaussian FWHM kernel (*3dmerge*) and normalized to percentage change from the mean signal, which was rescaled to be 100, from each voxel within a volume (*3dTstat* and *3dcalc*). Consequently, beta weights fitted to these scale data captured the maximal extent of BOLD signal variability within subjects relatively to the mean 100 (i.e., percentage of signal change).

Univariate Activation Analysis of fMRI Data. Preprocessed functional data were then compared across experimental conditions following a monotonic linear contrast for high (+0.75), medium (+0.25), low (-0.25), and control (-0.75) conditions using a generalized linear model in *3dREMLfit* for each participant (first-level analysis), after controlling for variance in head motion (*regress_apply_mot_types* demean deriv). In addition, time points in which significant motion events occurred (movement exceeded about 3° of rotation or 3 mm of translation in any direction relative to prior acquisition ± 1 time point) or excessive number of voxels that were considered as outliers (more than 10%) were censored from analyses (*regress_censor_motion* 0.3; *regress_censor_outliers*

0.1). That said, excluding the motion correction procedure in general yielded comparable results. Group-level statistics were then calculated using *3dMEMA*. The statistical threshold was determined by using *3dClustSim* to estimate the cluster-size threshold for a given voxel-wise *p*-value considering the actual smoothness and reconstructed voxel size of the EPI data (*regress_est_blur_epits*). Based on this simulation, significance level α was set as .01 after the correction of multiple comparisons, which was equivalent to uncorrected *p* values smaller than .005 with a cluster size of at least 55 voxels. A stricter corrected α level was chosen here because prior knowledge about the involved brain regions for task demands on visual WM precision was relatively limited.

Psychophysiological Interaction (PPI) Analysis. PPI analysis was performed to examine the correlational structures across brain regions in relation to the hippocampal sensitivity to task demands on WM precision. This analysis examined the effective connectivity between brain regions after partialling out the main effect difference in brain activities across experimental conditions (Cisler, Bush, & Steele, 2014; McLaren, Ries, Xu, & Johnson, 2012). Thus, PPI results were independent of that from the univariate activation analysis. In this analysis, left hippocampus was chosen as a seed region based on the results from the whole-brain activation analysis. Given potentially different structural and function connectivity of the anterior and posterior hippocampus with other brain regions (Poppenk, Evensmoen, Moscovitch, & Nadel, 2013), we conducted the PPI analysis separately using left anterior hippocampus (aHPC) and left posterior hippocampus (pHPC) as seed regions. In brief, the anterior and posterior parts of the hippocampus were identified using a coordinate-based segmentation approach based on

the location of uncal apex in the MNI (y = -21) neuroanatomical atlas (Poppenk et al., 2013). The average time series of a region of interest (ROI) was then extracted and de-convoluted based on the canonical hemodynamic function to obtain the underlying "physiological" time series. This "physiological" variable then multiplied with the time series of an experimental condition ("psychological" variable) to produce an interaction term for the given experimental condition. These psychophysiological interaction terms were then included in the analysis that was similar to the previous univariate activation analysis using *3dREMLfit* for each participant. Group-level analysis was then combined for group analysis using *3dMEMA* with a linear contrast capturing functional connectivity between brain regions and hippocampal ROIs across experimental conditions (i.e., +0.75, +0.25, -0.25, and -0.75). Based on the contrast analysis, a positive PPI result would suggest an increase in functional connectivity between a brain region and hippocampal ROIs as mnemonic precision load increases from perceptual/motor control condition to low, medium, and then high memory conditions, and vice versa.

Several aspects of the PPI analysis should be noted. First, the interaction term can capture the association between the seed region and a target region under experimental influences, or the effect of experimental condition on a target region under the influence of the seed region (Friston, 2011). Although these two interpretations are both possible, the former is more biologically plausible. Second, the PPI analysis includes several more predictors in the analysis, and thus is less power-efficient (Cisler et al., 2014). Thus, a more liberal criterion ($\alpha = .05$) was applied to determine significance after the correction of family-wise errors in the current study (e.g., Reagh et al., 2017). Specifically, group-

level results were corrected to a α level as .05, equivalent to p smaller than .05 with a cluster threshold of at least 150 contiguous voxels based on *3dClustSim*.

Results and Discussion

Behavioral Results. Of primarily interest, as summarized in Figure 4a, participants seemed to retain a comparable amount of information across different precision load memory conditions, as indicated by comparable tails of the recall error distributions across conditions. Repeated-measured ANOVAs on Pm showed a non-significant difference across the three memory conditions, regardless of whether only the trials performed inside the scanner (100 trials per condition per subject) were included in data analysis ($F_{(2, 38)} = 1.79$, $p = .18$, $\eta^2_p = .086$) or all the trials from inside and outside the scanner (150 trials per condition per subject) were included in data analysis ($F_{(2, 38)} = 2.43$, $p = .10$, $\eta^2_p = .114$). These results were consistent with a model-free data analysis approach by directly comparing the last three bins on each side of the recall error distribution across conditions using a Chi-squared test (all $ps > .10$). These results, along with the constant number of memory items across different precision load conditions, suggest that differences across experimental conditions may be unlikely driven by differences in visual WM capacity.

Univariate fMRI Results. As summarized in Figure 5 (also see Table 1), a univariate whole-brain activation analysis revealed several key brain regions that monotonically changed in BOLD activity in response to the precision load manipulation. Specifically, at a relatively conservative threshold (p corrected to .01 level), univariate analysis revealed significant regions of activation following the manipulation of

mnemonic precision across conditions (predefined contrast: +0.75, +0.25, -0.25, -0.75, for high, medium, low, and control conditions, respectively), including the left hippocampus-amygdala complex, left precuneus, bilateral middle prefrontal cortex, and bilateral angular gyrus (see Table 1 for details in MNI coordinates and voxel sizes). These regions were commonly reported in the literature to support the encoding/retrieval of episodic LTM representation with high fidelity for real-life objects (Reagh et al., 2017; Reagh & Yassa, 2014; Richter et al., 2016).

PPI Results. Experiment 2 further examined how the hippocampus was functionally connected with other brain regions as a function of the encoding precision manipulation using psychophysical interaction (PPI) analysis. Specifically, given that the anterior and posterior parts of the hippocampus may structurally and functionally connect with other brain regions in different ways (Poppenk et al., 2013; Strange, Witter, Lein, & Moser, 2014), the PPI analysis was conducted using the left anterior hippocampus (aHPC) and the left posterior hippocampus (pHPC) as separate seeds. After partialling out the main effect of precision load on fMRI BOLD signals, as shown in Figure 6, pHPC was positively associated with bilateral mPFC and superior parietal lobule (SPL) as WM precision load increased (see Table 2 details in MNI coordinates and voxel sizes). In contrast, aHPC was negatively associated with the left anterior cingulate cortex (ACC) and the right putamen, as WM precision load increased. These findings seem to be in line with some previous demonstrations of the dissociable functional connectivity (Di Martino et al., 2008; Reagh et al., 2017; Strange et al., 2014) and differentiable structural connection (M. Li, Long, & Yang, 2015; Poppenk et al., 2013; Preston & Eichenbaum,

2013) of aHPC versus pHPC with other brain regions. These dissociable connectivity effects may reflect different contributions of various structures (e.g., frontal-striatal circuit vs. frontal-parietal pathway) in the memory network to WM representations (Nee & Brown, 2012), potentially including to the precision aspect of WM. This speculation needs to be systematically tested in future research.

Experiment 3: Working Memory Precision Related Neural Activity Across Hippocampal Subfields

Method

Participants. Another eighteen right-handed participants (22.92 ± 3.06 years old, 11 females), normal color vision and normal (or corrected-to-normal) visual acuity were recruited from the Orange County community, Irvine, CA for Experiment 3. These participants reported no history of neurological or psychiatric disorders and no history of psychostimulant use. All participants provided written informed consent following the procedure approved by the Institutional Review Board of both the University of California, Irvine and University of California, Riverside, and they received monetary compensation for their participation.

Behavioral Task. The behavioral stimuli and task procedure were identical to Experiment 2.

MRI Data Acquisition. Neuroimaging data were acquired using the same scanner as that in Experiment 2. The scanning protocol was adapted to enable high-resolution fMRI data acquisition for the temporal region of the brain. The scanning sequence was as follows. First, the MP-RAGE structural scan protocol was the same as

Experiment 2. Second, a high-resolution functional scan protocol was used with these following parameters: TR = 2500 ms, TE = 26 ms, flip angle = 70 degrees, 37 slices, 160 dynamics per run, 1.8 × 1.8 mm^2 in-plane resolution, 1.8 mm slice thickness with a 0.2 mm gap, FOV = 180 mm × 74 mm ×180 mm. The timing of the behavioral task and functional scans (7 functional runs, each lasting for 6 minutes and 40 seconds excluding 4 initial dummy scans) were kept the same as that in Experiment 2.

MRI Data Preprocessing. The neuroimaging data preprocessing protocol with AFNI (Cox, 1996) was mostly similar to that in Experiment 2 with some modifications for ROI analysis of high-resolution fMRI data in the native (subject) space. Briefly, functional data were despiked (*3dDespiked*), slice timing corrected (*3dtshift*), co-registered to the structure scan (*align_epi_anat.py*), motion corrected (*3dvolreg*), blurred to 2 mm isotropic (*3dmerge*) with a Gaussian FWHM kernel, and masked to exclude voxels outside the brain (*3dautomask*). We then obtained models of ongoing BOLD activity per subject using the same univariate analysis procedure as detailed in Experiment 2 (*3dREMLfit*).

Anatomical Hippocampal Subfield ROI Segmentations. Hippocampal subfield segmentation was implemented using a joint label fusion (JLF) approach (H. Wang et al., 2015) based on a set of 17 atlas sets. Each of these atlas sets consists of a T1-weighted image (0.75 × 0.75 × 0.75 mm^3), a T2-weighted image (0.47 × 0.47 × 2 mm^3) angled perpendicular to the long axis of the hippocampus (see Yushkevich et al., 2010 for details), and a set of manually annotated labels for bilateral hippocampal subfields, including DG/CA3, CA1, and subiculum (defined in the space of the corresponding T2

image). DG and CA3 subfields were combined as a single label because of the uncertainty in separating signals from these two subfields in later fMRI data even at 1.8 × 1.8 mm^2 in-plate resolution (Reagh et al., 2017).

JLF was performed in a T1-weighted image for individual participants by warping each atlas (T1-weighted image + label set) to individual-specific T1-weighted images using the open-source software, Advanced Normalization Tools (ANTs, http://stnava.github.io/ANTs/). Prior to this warping, the target individual-specific T1 image was preprocessed with bias correction (Tustison et al., 2010), skull stripping (Tustison et al., 2014), and de-noising (Manjón, Coupé, Martí-Bonmatí, Collins, & Robles, 2009) procedures. After these preprocessing steps, JLF performed a weighted voting at each voxel based on a patch-based intensity similarity while minimizing the informational redundancy between atlas contributions. To minimize the number of registrations required for JLF, an optimal shape/intensity template (Avants et al., 2010) was generated offline from the set of 17 atlas sets using an pseudo-geodesic approach (Tustison & Avants, 2013). The rigid transform between the atlas T1/T2-weighted image pairs (Avants et al., 2014) was also further calculated offline. Using the atlas-based set of T1/T2 rigid transforms and the T1/template non-linear transforms, transformation between the target individual-specific T1-weighted image and the atlas T1-weighted template was calculated to warp the entire set of atlas labels and T1-weighted images to the target subject for subsequent JLF.

Hippocampal Subfield ROI Analysis. Extracted BOLD signals were compared using contrast analysis procedures as previously described (also see Rosenthal, Rosnow,

& Rubin, 2000 for details). That is, instead of omnibus ANOVAs, we directly tested the *a priori* hypothesis that a brain region sensitive to task demands on WM precision should follow a monotonic decreasing pattern in response to the high-precision (+1), medium-precision (+0), and low-precision (-1) conditions, after subtracting out the individual differences in the perceptual/motor control condition. Since there was no significant hemisphere by precision load condition interaction (all *ps* > 0.10), data from different hemispheres were combined for each hippocampal ROI. Therefore, in the following analyses, subfield location (i.e., DG/CA3, CA1, and subiculum) was treated as a factor to examine whether there was an interaction between the location of the hippocampus and the task-related monotonic pattern of the BOLD signals.

Results and Discussion

Behavioral Results. Participants' behavioral performance in Experiment 3 was consistent with that in Experiment 2, as summarized in Figure 4b. That is, participants retained a comparable amount of information across different precision load memory conditions, as suggested by repeated-measures ANOVAs on Pm estimated from the trials (100 trials per condition) during the scanning session ($F_{(2, 34)} = 0.45$, $p = .64$, $\eta^2_p = .026$) and all trials collected during and before the scanning sessions (150 trials per condition in total, $F_{(2, 34)} = 2.08$, $p = .14$, $\eta^2_p = .109$). Again, analyses with the model-free approach of directly comparing the last three bins on each side of the recall error distribution across conditions using a Chi-squared test also yielded similar findings (all *ps* > .10). Overall, participants' performances in Experiment 2 and 3 seem to be comparable.

Activities of Hippocampal ROIs. BOLD signals in DG/CA3 seemed to decrease monotonically in response to the precision load manipulation after correcting for the baseline offset in the perceptual/motor control condition (see Figure 7). This pattern was supported by a significant linear contrast across memory conditions ($F_{(1, 17)} = 5.20$, $p = .036$, $\eta^2_p = .234$). In comparison, the BOLD signals in the CA1 and subiculum were not significantly modulated by precision load manipulation ($Fs < 1$). These observations were further supported by a significant interaction between the linear contrast of the BOLD signals between DG/CA3 and CA1 ($F_{(1, 17)} = 7.30$, $p = .015$, $\eta^2_p = .300$) and between DG/CA3 and subiculum ($F_{(1, 17)} = 4.55$, $p = .048$, $\eta^2_p = .211$). These results therefore suggest that the precision-related hippocampal activity may be attributed to the DG/CA3 subfield, instead of the CA1 or the subiculum.

General Discussion

Experiment 2 and 3 have demonstrated that the hippocampus, especially its DG/CA3 subfield, could track the task demands on WM precision. That is, as the task demand on WM precision increases, hippocampal activities also increase accordingly, potentially to engage pattern separation computation in the DG/CA3 to disambiguate overlapping mnemonic representations to ensure a certain level of precision for optimal task performance.

However, this interpretation may be complicated by the lack of significant behavioral precision effects due to the precision manipulation, although this is a replication of previous findings using similar manipulation (Zhang & Luck, 2009; 2011). As previously mentioned, it is difficult to precisely estimate the precision parameter in

the color spokes conditions (i.e., medium and low precision load conditions). Specifically, each spoke (response option) covers 24 and 60 degrees in the 15-spoke and 6-spoke conditions, respectively, setting a limit on the ability to estimate SD as determined by the Nyquist–Shannon sampling theorem.

Another potential problem with the current findings is that the monotonic increase in hippocampal activity due to the precision load manipulation could result from increases in cognitive effort instead of increases in the task demands on precision. That is, although recall performance is comparable across the three precision load conditions in both experiments, participants may devote more efforts in the high-precision load condition, as compared to lower-precision load conditions, simply because the high load condition is more demanding (Kurzban, Duckworth, Kable, & Myers, 2013).

It is thus pivotal to demonstrate that hippocampal activities can be directly linked to the behavioral measure of WM precision. To evaluate this possibility, we tested whether hippocampal activities could predict WM precision from the high-precision load condition in which WM precision could be more accurately estimated (Zhang & Luck, 2008) .To keep consistency between Experiment 2 and 3, this analysis focused on the activity of the whole left hippocampus (similar results were obtained when bilateral hippocampi were combined) and its correlation between WM precision. The whole left hippocampal ROI was determined anatomically based on *Freesurfer* labels. To correct for individual differences in baseline neural activities, overall hippocampal activation in the high-precision WM task was defined as the difference in the beta values in the high-precision load condition relative to the perceptual/motor control condition ($B_{High\text{-}Control}$).

The correlation between the behavioral measure of WM precision (SD in the high-precision load condition) and the hippocampal activation level ($B_{High\text{-}Control}$) was first computed separately for each experiment and then combined meta-analytically, instead of simply aggregated, to avoid the Simpson paradox (H. Cooper & Patall, 2009).

As shown in Figure 8, in both Experiment 2 and 3, participants with higher WM precision (smaller SD) in the high-precision load condition tended to have greater hippocampal activation levels ($B_{High\text{-}Control}$). Although this correlation was not statistically significant in Experiment 2 (r = -.23, p =.17, n = 20), it was statistically significant in Experiment 3 (r = -.48, p =.016, n = 18). After combining these two correlations meta-analytically in a fixed-effect model to increase statistical power (n = 38), there was a significant correlation between behavioral estimates of WM precision and hippocampal activation levels (r = -.35, p =.019). In contrast, hippocampal activity was not significantly correlated with Pm separately in each experiment (all ps > .20) or when results from two experiments were meta-analytically combined (r = -.03, p =.42).

Together, this robust association between hippocampal activity and WM precision provides strong evidence supporting the critical role of the hippocampus in retaining precise WM representations. It also addresses the two potential concerns of the main findings. First, hippocampal activity is predictive of WM precision across subjects, even though the significant effects of the precision manipulation on hippocampal BOLD activity may not lead to significant behavioral effects. Second, the correlation between hippocampal activation and overall WM precision is obtained from a memory condition (i.e., the high-precision load condition) relative to the control condition, ruling out the

alternative effort account that attributes the significant effects on hippocampal BOLD activity to changes in efforts across different WM conditions.

Conclusion

Findings from Experiment 2 and 3 have provided direct evidence for the contribution of the hippocampus to WM precision in that 1) BOLD activity in the hippocampus – especially its DG/CA3 subfield that has been implicated in pattern separation – increases with the task demands on WM precision; and 2) hippocampal activity can predict WM precision, but not WM capacity, across subjects. These findings are unlikely due to LTM's involvement as argued by some previous studies (Jeneson et al., 2011; 2012), given the short delay interval (i.e., 1.8 seconds) and the reasonable memory set size (i.e., 4 colors) in the current experiments.

Chapter 5.

Decoding Precise Item-specific Working Memory Representations from Hippocampal DG/CA3

The elevated hippocampal activation in response to the increased task demands on WM precision in Experiment 2 and 3 implies that the hippocampus is involved in retaining precise WM representations, in line with some previous findings suggesting hippocampal involvement in WM (Ranganath & Blumenfeld, 2005; Yonelinas, 2013). However, these fMRI activation-based effects do not necessarily mean that WM information is retained in the hippocampus. These effects, for example, could be a manifestation of top-down modulation of hippocampal activity from the prefrontal cortex due to increased cognitive load (E. K. Miller & Cohen, 2001). Furthermore, considerable evidence has been cumulating in the neuroimaging literature for the functional independence between fMRI BOLD effects and decoding effects in visual WM (Bettencourt & Xu, 2015; Ester, Sprague, & Serences, 2015; Harrison & Tong, 2009; Rose et al., 2016). For example, a given brain region such as the primary visual cortex can carry feature-specific information manifested as decodable representations using Multi-Voxel Pattern Analysis (MVPA), even when the same region does not show measurable effects in BOLD activity, or vice versa (Harrison & Tong, 2009; Serences, Ester, Vogel, & Awh, 2009). One possibility is that fMRI BOLD and decoding effects may reflect different memory states (Stokes, 2015) that are supported by different

underlying neural mechanisms (e.g., sub-threshold synaptic activities versus spiking activities, Rose et al., 2016).

Thus, beyond the fMRI BOLD evidence supporting hippocampal involvement in WM precision, Experiment 4 in this chapter will try to decode trial-by-trial item-specific WM content from the hippocampal DG/CA3 subfield. To achieve this goal, Experiment 4 will take advantage of two methodological innovations.

First, Experiment 4 adopts a novel Inverted Encoding Model (IEM) approach to decode trial-by-trial item-specific information retained in visual WM. This method leverages rich neurophysiological knowledge about neural population coding (i.e., how a population of neurons encodes simple object features, such as orientations, colors, and spatial locations) to decode feature-specific information from the overall neural response profile captured by fMRI BOLD signals. Specifically, based on findings using single unit recordings, we can assume that a simple surface feature (e.g., orientation) may be encoded by a pool of feature-selective neurons (captured by different voxels in the fMRI data), each of which is tuned to a specific feature value (i.e., *encoding model*). Observed overall neural response profile elicited by a specific feature (e.g., 30-degree orientation) can be considered a weighted summation of activities from these different groups of feature-specific neurons (voxels), forming a bell-shaped distribution along the entire feature space (e.g., -90 to +90 degrees). Based on this population encoding principle, it is possible to estimate how these different groups of feature-specific neurons (voxels) contribute to overall response profiles with different *weights*. We may then approximate which feature value is encoded by a neuron population by applying the estimated weights

to its overall neural response profile at a different time point (i.e., *inverted encoding model*). Using this method, previous studies have identified a set of distributed brain regions containing item-specific information during the delay period of a visual WM task (e.g., Ester et al., 2015). For instance, orientation representations in visual WM can be recovered from fMRI BOLD activities sampled at a coarser spatial resolution (3 mm^3 voxel) in the visual, parietal, and prefrontal regions of the brain (Ester et al., 2015; Harrison & Tong, 2009), even though orientation selectivity primarily resides at finer spatial scales (e.g., columns of neurons) in the visual cortex. However, due to complicated folding and reduced number of voxels (at 3 mm^3 resolution) in the hippocampus, conventional fMRI protocols in previous studies were unable to reveal significant hippocampal contributions to decodable visual WM content (Ester et al., 2015).

Thus, second, a new MRI sequence will be used to get more optimal signals with higher in-plane resolution (1.5×1.5 mm^2) for partitioning hippocampal subfields. In addition, This high-resolution fMRI protocol is also important for decoding analysis, because decoding relies on multivariate patterns instead of overall average BOLD signals such that an reasonably increased number of voxels due to reduced voxel size may boost decoding accuracy (Haynes, 2015). Together, by combining a novel IEM approach and a state-of-the-art high-resolution fMRI sequence, Experiment 4 may thus provide a better evaluation for the prediction that the hippocampus, especially its pattern separation related DG/CA3 subfield, contains item-specific information retained in visual WM.

Experiment 4: Decoding Working Memory Content in Hippocampal Subfields Using Inverted Encoding Model and High-resolution fMRI

Method

Participants. A new group of 16 participants (8 females, on average 21.62 ± 3.06 years old) were recruited from University of California, Riverside campus for Experiment 4 with monetary compensation. This sample size is determined according to previous studies using similar methods (e.g., Sprague, Ester, & Serences, 2014; Ester et al., 2015). All participants reported normal color vision, normal (or corrected-to-normal) visual acuity, no history of neurological or psychiatric disorders, and no previous or recent psychostimulant use. All participants provided written informed consent following the procedure approved by the Institutional Review Board of the University of California, Riverside.

Behavioral Task. Experiment 4 adapted an orientation WM task that has been previously established in several studies for decoding item-specific information (orientation in this case) using the IEM method (Ester et al., 2015; Serences et al., 2009). The use of orientation instead of color is to follow practice from previous studies (Ester et al., 2015; Harrison & Tong, 2009; Serences et al., 2009), and to generalize the findings of Experiment 2 and 3 from color to another feature dimension that is also void of strong LTM influence (e.g., orientation). Specifically, in this orientation WM task (Figure 9), two sine-wave gratings (radius: 4.5°, contrast: 80%, spatial frequency: ~1 cycle per degree in visual angle, randomized phase) were sequentially presented at the center of the screen on each trial. Each of the grating stimuli was presented on the screen for 200 ms

with a 400-ms blank screen in between. They were oriented at different orientations that were randomly sampled from 9 possible predefined orientations (0 to 160° in 20° increments) with a small angular jitter at presentation (±1° to 5°; randomly chosen on each trial). A digit cue ("1" or "2") appeared 400 ms after the offset the second grating and stayed on the screen for 550 ms to indicate which gating orientation should be remembered over the delay period (8750 ms). Participants were asked to retain only the cued grating and ignore the other grating. After the delay period, a test grating starting at a random orientation was presented on the screen. Participants used button presses to adjust the orientation of the test grating with similar visual attributes as the to-be-remembered grating but starting at a random orientation to reconstruct the to-be-remembered orientation of the cued grating from WM. Specifically, they used the right index finger to press a button to rotate the grating clockwise and the right middle finger to press a button to rotate the grating counter clockwise. They were asked to make a response within 3500 ms following the onset of the test grating, and the orientation of the test grating at the end of this interval was taken as the participant's final response. Visual feedback was presented at the end of the response interval by presenting a bar outside the test grating at the correct orientation of the to-be-remember grating. Different trials were separated by a random inter-trial interval that lasted for 3500 ms or 5250 ms (randomized across trials). All participants completed 10 blocks with 18 trials in each block. All experimental factors, namely the position of cue item (first or second items) and the orientation of presented gratings, were randomly intermixed within each experimental

block. Participants' recall errors across trials were analyzed using the Zhang and Luck (2008) model as previously described.

MRI Data Acquisition. Neuroimaging data were acquired on a 3.0 Tesla Siemens Prisma scanner, using a 32-channel sensitivity encoding (SENSE) coil at the Center for Advanced Neuroimaging at the University of California, Riverside. Scanning sequence was optimized for high-resolution functional MRI with whole-brain coverage. Specifically, following a MP-RAGE structural scan (0.8 mm isotropic voxels) at the beginning an experimental session, 10 functional runs were acquired with these following settings: TR = 1750 ms, TE = 32 ms, flip angle = 74°, 69 slices, 189 dynamics per run, 1.5×1.5 mm^2 in plane resolution with 2 mm gap, FOV read = 222 mm, FOV phase = 86.5%. Each functional run lasted 5 minutes and 30.75 seconds excluding initial dummy scans acquired to ensure T1 signal stabilization. In addition, following the last functional run, two additional functional scans with opposite phases were acquired for correction of EPI distortions (Irfanoglu et al., 2015).

fMRI Data Preprocessing and Hippocampal Subfield ROI Extraction. The neuroimaging data preprocessing protocol was comparable as the previous experiments except for the inclusion of correction for EPI distortions (Irfanoglu et al., 2015). Specifically, functional data were despiked (*3dDespiked*), slice timing corrected (*3dtshift*), reverse-blip registered (*blip*), aligned (*align_epi_anat.py*), and motion corrected (*3dvolreg*). To avoid introducing artificial auto-correlation in later decoding analysis, functional data were not smooth and were kept in original grid size ($1.5 \times 1.5 \times 2$ mm^3). The same anatomical hippocampal subfield segmentation protocol was used as

Experiment 3. Again, DG and CA3 subfields were grouped as a single ROI. Bilateral hippocampal ROIs were combined for later analysis as Experiment 3.

Inverted Encoding Model. This analysis was implemented to explicitly examine whether a brain region contain item-specific information regarding the to-be-remember orientation from the average fMRI signals in the last 3 TRs of the visual WM delay period (Figure 9). This time window was chosen to minimize signals primarily due to visual perceptual processing of the task stimuli (Ester et al., 2015). For the IEM, a linear encoding modeling was first used to construct orientation-selective response in each predefined ROIs as previously described in Ester et al. (2015). In brief, the response of each voxel in a ROI was assumed to be a linear summation of 9 idealized information channel (9 smooth sinusoids as detailed in Ester et al., 2015). That is, observed signals from raw EPI data (without deconvolution), **B** (m voxels × n trials), would be a weighted summation of predicted responses, **C** (k channels × n trials), for each information channel on each trial with a set of weights **W** (m voxels × k channels), namely,

$$\mathbf{B} = \mathbf{WC}$$

The predicted responses **C** were estimated by a set of base function consisting of 9 half-wave rectified sinusoids centered at different orientations to approximate the tuning profile of orientation sensitive neurons (Ringach, Shapley, & Hawken, 2002). Given $\mathbf{B_1}$ and $\mathbf{C_1}$ from a set of training dataset, the weight matrix was further estimated as

$$\widehat{\mathbf{W}} = \mathbf{B_1}\,\mathbf{C^T_1}\,(\mathbf{C_1}\,\mathbf{C^T_1})^{-1}$$

These weights were then applied to an independent test dataset, in which the observed signals $\mathbf{B_2}$ and the weights $\widehat{\mathbf{W}}$ were used to calculate the channel responses in these observed data using ordinary least-squares regression,

$$\mathbf{C_2} = (\widehat{\mathbf{W}}^{\mathrm{T}}\,\widehat{\mathbf{W}})^{-1}\widehat{\mathbf{W}}^{\mathrm{T}}\,\mathbf{B_2}$$

A "leave-one-out" cross-validation routine was used to obtained reliable estimate channel responses for all trails in the experiment based on independent datasets (Figure 9). Specifically, in every iteration, all but one experimental blocks were treated as $\mathbf{B_1}$ for the estimation of $\widehat{\mathbf{W}}$, while the remaining block was treated as $\mathbf{B_2}$ for the estimation of $\mathbf{C_2}$. This analysis yielded estimated channel responses $\mathbf{C_2}$ for all experimental trials. These estimated channel responses $\mathbf{C_2}$ were then shifted to center at 0° and averaged across trials, forming a bell-shaped channel response pattern when decoding was successful (Figure 9).

Statistical significance of the reconstructed representations of the to-be-remembered orientation, to-be-forgotten orientation, and the difference between these two was evaluated using a bootstrapping method. Specifically, the average reconstructed representations of a random sample from the recruited subjects (with replacement) were fitted to an exponential cosine function (see Ester et al., 2015 for details), yielding an estimate of the tuning function amplitude. This procedure was repeated 2000 times, yielding an empirical distribution of amplitude estimates based on the observed data. Whether a given ROI contained item-specific information regarding the to-be-remembered/to-be-forgotten orientation was evaluated by the proportion of resampled amplitude estimates that was greater than 0 ($\alpha = 0.05$, one-tailed). Here, one-tailed tests

were used because negative reconstructed tuning amplitudes were less interpretable (Ester et al., 2015). Similar approach was used to evaluate whether amplitude estimates were higher for the to-be-remembered relative to to-be-forgotten orientations by computing the amplitude estimates based on the difference score between these two reconstructed representations (Ester et al., 2015).

Searchlight Analysis. With whole-brain high-resolution fMRI, a roving searchlight procedure in combination with the IEM analysis was performed to further identify other brain regions that contained item-specific information regarding the to-be-remembered orientation. First, before the searchlight analysis, individual structural data were normalized to a common space using a high-resolution MNI template (0.8 mm isotropic voxels) using the ANTs that applied multi-step nonlinear diffeomorphic transformations (Avants et al., 2008). Parameters from these transformations were also used to transform functional data into the template MNI space for later group-level comparison (e.g., Reagh et al., 2017). Second, in the subsequent searchlight analysis, roving spherical clusters (8 mm radius) centered on each voxel in a cortical mask containing only gray matter voxels for each participant (Ester et al., 2015) were used to decode item-specific information from the averaged fMRI BOLD signals in the last 3 TRs of the delay period in each trial. Specifically, for each searchlight sphere, IEM analysis was repeated to estimate the responses of nine hypothetical orientation channels corresponding to the to-be-remembered orientations and to fit the resulting reconstructions (i.e., amplitude of the tuning fitted tuning curve) with the approach described before. Spheres with fewer than 100 voxels were discarded, yielding an

average cluster size of 209 voxels (with a maximum size of 257 voxels). Last, group-level results were evaluated by calculating a one-sample *t*-test at each voxel (*3dMEMA*) to identify regions that robustly contained item-specific information regarding the to-be-remembered orientation during WM delay period (Ester et al., 2015). The decodability map measured by group-level *t* values was then projected to a cortical surface in the MNI space. Based on a simulation using *3dClustSim*, significance level α was set as .05 (one-tailed) after the correction of multiple comparisons based on the actual smoothness level of the data, which was equivalent to uncorrected one-tailed *p* values smaller than .05 with a cluster size of at least 40 voxels.

Granger Causality Analysis. This analysis was to reveal the functional dynamics between the hippocampus and the visual cortex, where robust reconstruction of item-specific information during visual WM retention interval has been reported in the literature studies (Ester et al., 2015; Harrison & Tong, 2009; but see Bettencourt & Xu, 2015). Granger causality analysis is an exploratory method that can be used to study directional influences between different brain regions (Deshpande, LaConte, James, Peltier, & Hu, 2009). The idea is that, if past values of time series X can predict the current and future values of time series Y, then a directional causal influence from time series X to time series Y can be inferred (Granger, 1969). The present analysis protocol was modified based on previous studies (e.g., Sathian, Deshpande, & Stilla, 2013; Deshpande et al., 2009).

First, BOLD signal time series were averaged and extracted from different ROIs. Here, the hippocampal DG/CA3 ROIs were analytically based on the segmentation

procedure as previously described. The visual cortex ROIs were functionally defined as spheres with an 8-mm radius centered at the cluster (i.e., center of mass) containing robust reconstructed visual WM representations in bilateral occipital lobes based on the group-level searchlight results. Second, ROI-specific Hemodynamic Response Functions (HRFs) related to WM delay period were then estimated based on a robust inverse-logit method (Lindquist & Wager, 2007). Third, neural signals related to information maintenance in WM were then extracted by deconvolving the raw BOLD signals based on the ROI-specific HRFs using a Weiner filter (Glover, 1999). Fourth, pair-wise Granger causality analysis was conducted based on the deconvolved BOLD time serials using a first order dynamic multivariate autoregressive (MVAR) model (i.e., using time point t to predict maximally only the next time point, $t + 1$, with the temporal gap as 1 TR = 1.75s). Here, the first order model was applied because causal influences arising from neural delay often occur less than 1 TR. The order of 1 in the MVAR may thus be the best approximation for the underlying neural connectivity based on the nature of the observed fMRI data (Feng et al., 2015; Goodyear et al., 2017). Fifth, the resulting effective connectivity values of each trial during the delay period were then averaged across the last 3 TRs of the delay period to match with those selected for IEM analysis. A positive value indicates that BOLD signals between two regions change in the same direction during these 3 TRs; whereas, a negative value means that BOLD signals between two regions change in the opposite direction during these 3 TRs. Last, these values were then further compared against with 0 across trials for each participant using a one-sample t-test (two-tailed due to unknown direction) to reveal whether the effective

connectivity during WM retention significantly deviated from 0 (theoretically null value). The directional Z values based on p values (uncorrected) estimated from each subject for each pair of ROIs were then combined using Stouffer's Z-score method for group-level analysis, equivalent to a fixed-effect meta-analysis across 16 subjects (Goh, Hall, & Rosenthal, 2016; Rosenthal & DiMatteo, 2001). The meta-analytically combined p-values at the group level were then Bonferroni corrected to adjusted for pair-wise multiple comparison.

Results and Discussion

Behavioral Performance. As summarized in Figure 10a, the overall performances in this task was highly accurate (Pm = 95%, std. = 5%; SD = 13.23^{o}, std. = 2.29^{o}). Critically, task performance in terms of Pm or SD did not seem to vary with the order of the test item (*p*s > .30). That is, regardless of whether the test item was presented as the first or second item, participants performed equally well.

Hippocampal ROIs. Using the IEM method (Sprague et al., 2014; Sprague, Ester, & Serences, 2016), Experiment 4 tested whether activity patterns during the delay period in hippocampal subfields could predict which of the two orientations was held in visual WM. For each hippocampal subfield ROI (DG/CA3, CA1, and Subiculum), reconstructions of the remembered and non-remembered orientation from hippocampal subfields are plotted in Figure 10b. We obtained robust reconstructed representations for the remembered orientation ($p < .0005$, one-tailed), but not for the non-remembered orientation ($p = .53$, one-tailed), from the DG/CA3 subfield. Critically, reconstruction amplitudes were reliably higher for the remembered relative to the non-remembered

orientation in the DG/CA3 subfield ($p = 0.005$, one-tailed). In contrast, signals from hippocampal CA1 and subiculum subfield failed to show robust reconstruction of the remembered orientation ($ps > .13$, one-tailed). Note, although CA1 had a larger number of voxels (range: 625 to 1006), the numbers of voxels in the DG/CA3 (range: 262 to 379) and subiculum (range: 255 to 430) ROIs were more or less comparable. The observation of better decodability in DG/CA3, therefore, could not be attributed to an advantage stemming from larger numbers of voxels for decoding analysis (Haynes, 2015).

In fact, when all hippocampal voxels across hemispheres were combined to increase the number of voxels, hippocampal decodability for visual WM content was not improved (Figure 10c). This whole-hippocampal ROI has yielded similarly poor decoding performance as that in an adjacent control region, the amygdala, which might not be sensitive to emotionally-neutral visual features (e.g., orientation). This lack of decodability in the bilateral whole hippocampi might be related to the complicated folding structures in the hippocampus, which could add heterogeneity in neural signals that compromised decoding performance. Hence, using high-resolution fMRI to separate subfield specific signals may thus be critical to reveal hippocampal contribution to visual WM representation and/or retention.

Searchlight Analysis. Beyond the hippocampus, reconstructions of the remembered orientation across other areas of the brain were also evaluated using a searchlight analysis (Ester et al., 2015). This analysis showed highly consistent findings as previous studies (Bettencourt & Xu, 2015; Ester et al., 2015; Harrison & Tong, 2009), such that widely distributed brain regions, including frontal, parietal, and occipital

cortices, contained decodable item-specific information for the remembered orientation (see Figure 11 and Table 3).

Granger Causality Analysis. Given the robust decoding results in the visual cortices that are consistent with some previous findings (Ester et al., 2015; Harrison & Tong, 2009), it is of great interest to examine the dynamic relationship between signals in the hippocampal DG/CA3 subfield and those in the visual cortex during the visual WM delay period. As shown in Figure 12, signals in the hippocampal DG/CA3 subfield could robustly predict signals in the ipsilateral visual cortex ROIs at a later time point during the WM delay period (ps < .0001, after Bonferroni correction). Although left visual cortex ROI also contained information that was predictive of that in the left hippocampal DG/CA3 (p = .0003, after Bonferroni correction), the overall dynamic connectivity was stronger from the hippocampus to the visual cortex than that from the visual cortex to the hippocampus. Specifically, for each subject on each trial, two average effective connectivity values were separately calculated to represent the overall dynamic connection from the hippocampus to the visual cortex and from the visual cortex to the hippocampus. A paired-sample t-test across trials was then calculated for each participant to evaluate whether these two effective connectivity values systematically differed from one another in terms of magnitude. The group-level results combined meta-analytically across individual tests showed that the average effective connectivity from the hippocampus to the visual cortex was substantially more robust, as compared to that from the visual cortex to the hippocampus (p < .0001). This directional pattern, although at a coarse temporal scale, may provide some support for the sensory recruitment hypothesis

(see a recent review in Scimeca, Kiyonaga, & D'Esposito, 2018), such that visual cortices may be recruited to support visual WM retrieval rather than being a region to maintain these representations. The current finding suggests that this sensory recruitment may be contingent on hippocampal DG/CA3 activity.

Conclusion

Using high-resolution fMRI and a multivariate IEM decoding method, Experiment 4 provides by far the first evidence that the hippocampal DG/CA3 subfield carries precise item-specific information retained in visual WM. Furthermore, signals in the hippocampal DG/CA3 also seem to occur earlier than signals in visual cortices, which contain item-specific information potentially due to a sensory recruitment mechanism (Harrison & Tong, 2009; Scimeca et al., 2018; Serences et al., 2009). Overall, these findings support the hippocampal pattern separation hypothesis for the retention of precise visual WM representations.

Chapter 6.

General Discussion

Summary of Findings

The dissertation research has demonstrated three lines of evidence supporting hippocampal pattern separation as a neurocognitive mechanism underlying the precision of retained WM representations (i.e., pattern separation hypothesis). First, at the behavioral level, estimates of mnemonic precision but not the probability of memory retrieval across WM and LTM are highly correlated with the estimate of pattern separation function in Experiment 1. These correlations suggest a substantial amount of shared variance among these measures, which may be related to a latent construct regarding memory quality or mental clarity.

Second, Experiment 2 has demonstrated that the increase in task demands on WM precision can lead to higher fMRI BOLD activity in the hippocampus, along with several other brain regions (e.g., prefrontal cortex, angular gyrus, and the precuneus). This hippocampal involvement may be further localized to DG/CA3 subfield (Experiment 3), where pattern separation computation most likely takes place. Critically, across individuals, higher hippocampal activation in the high-precision load condition (relative to the perception/motor control condition) is significantly associated with WM precision when all data are meta-analytically combined from Experiment 2 and 3 (n = 38). Together, these fMRI findings (i.e., increased hippocampal BOLD activities due to WM precision load and larger changes in hippocampal activity for more precise WM across

individuals) suggest that the hippocampus is a critical node in the brain network supporting precise WM.

Third, using a combination of whole-brain high-resolution fMRI and a novel IEM method, Experiment 4 shows that item-specific information for a simple surface feature (i.e., orientation) can be reliably decoded from the hippocampal DG/CA3 subfield, a hypothesized locus for pattern separation computation, among other previously reported regions, including the visual cortex, the prefrontal cortex, and the parietal cortex (Ester et al., 2015). This finding may rule out an alternative interpretation that the hippocampal findings in Experiment 2 and 3 reflect increases in perceived task difficulty (see more discussions in Chapter 4). The findings from Experiment 4 thus provide direct evidence that the hippocampus carries precise item-specific information in WM.

Together, these findings are in line with the hippocampal pattern separation hypothesis for WM precision. In addition, they shed light on the recent re-evaluation of the traditional system view of memory and on the recent debate regarding the nature of WM representations.

Functional Roles of the Hippocampus in Human Cognition

Early knowledge about the role of the hippocampus in human cognition comes from studies on neurological patients with MTL lesions (Scoville & Milner, 1957). These patients could carry on a coherent conversation, supported by temporary information maintenance in WM, but moments later were unable to recall that the conversation took place or to whom they spoke, indicating disrupted declarative LTM. These findings have provided strong support for the conventional system view of human memory, according

to which LTM and WM are independent memory processes/systems supported by different neural mechanisms (Squire, 1986). As such, *memory modulation hypothesis* postulates that the hippocampus primarily supports episodic LTM and uses LTM representations as a "currency" to interact with other cognitive processes (Shohamy & Turk-Browne, 2013). For example, the hippocampus can support transient information processing by reactivating related experiences from the past to make them available to active processes (Fortin, Wright, & Eichenbaum, 2004; Frankland & Bontempi, 2005; McClelland, McNaughton, & OReilly, 1995). Furthermore, it can support more permanent information processing by transferring active mental representations to more durable ones through of cortical and subcortical consolidation (McClelland et al., 1995; Takashima et al., 2006).

In contrast, an emerging *adaptive function hypothesis* argues that the hippocampus serves as a representational hub to support a certain aspect of mental representations/processes, as opposed to serving as a dedicated functional module reserved particularly for declarative LTM (Shohamy & Turk-Browne, 2013; Yonelinas, 2013). According to this hypothesis, the hippocampus – with specific physiological and computational properties including recurrence, sparse coding, rapid binding, and massive interconnectedness (Eichenbaum, 2014; Eichenbaum & Cohen, 2014; see summaries in Eichenbaum, Yonelinas, & Ranganath, 2007) – is useful for the processing of mental representations, irrespective of the time course and content of these representations. For example, beyond the blurred boundary between WM and LTM in the hippocampus (Kamiński et al., 2017), another line of research on implicit memory (e.g., Addante,

2015; Degonda et al., 2005) also challenges the established system view that the hippocampus only contributes to conscious/explicit mnemonic representations/processes (e.g., facts, daily episodes, etc.) but not to unconscious/implicit mnemonic representations/processes (e.g., conditioning, procedural skills, etc., Knowlton, Mangels, & Squire, 1996; Squire, 1986; Squire & Dede, 2015). Furthermore, pushing this boundary further, some recent studies have demonstrated hippocampal contributions to fine perceptual discrimination (Graham, Barense, & Lee, 2010; Lee, Yeung, & Barense, 2012; Lee, Barense, & Graham, 2005), primarily via the functional connection between the hippocampus and sensory cortices (e.g., Hindy, Ng, & Turk-Browne, 2016).

Nevertheless, the exact mental representations/processes that the hippocampus may contribute to WM remain unclear. On the one hand, some studies suggest that the hippocampus may be involved to support relational over item information in WM (see Yonelinas, 2013 for a review). Supporting this view, damage in the hippocampus can impair patients' WM task performance for complex events that require combining elements together, such as object-location binding (Olson, Moore, Stark, & Chatterjee, 2006), face-scene and object-scene relations (Hannula et al., 2006), and topographical stimuli (Hartley et al., 2007). On the other hand, whether the distinction between item versus relational information successfully identify qualitatively distinct forms of memory is still controversial (Squire, Wixted, & Clark, 2007; Wixted, 2007), because this distinction critically relies on behavioral differentiation between two forms of recognition (i.e., familiarity vs. recollection) under a dual-process framework (Yonelinas, 2002; Yonelinas et al., 2010; Yonelinas & Parks, 2007). Some recent studies have further

shown evidence against the distinction of item versus relational WM deficits in MTL-damaged patients (e.g., Squire, 2017).

The current dissertation research thus adds to this emerging literature with a novel precision account for the hippocampal involvement in WM. That is, the hippocampus supports precision of WM representation with its pattern separation computation in its DG/CA3 subfield. Previous findings regarding the hippocampus involvement in remembering complex stimuli may be critically related to increased demands on representational precision in these stimuli, as compared to much simpler stimuli. Supporting this precision load account, damages in the MTL including the hippocampus were found to impair WM precision (Zhang & Yonelinas, 2012), resembling findings of compromised performance for complex stimuli due to MTL damages in previous studies (Hannula et al., 2006; Hartley et al., 2007; Olson et al., 2006). Can this precision account also explain different task performances in item and relational memory reported in the literature (see Yonelinas, 2013 for a review)? One possibility is that the binding of multiple items in relational memory may reduce the precision of retained memory representation, due to the pooling of mnemonic variance. This is similar to the Signal Detection Theory interpretation of feature versus conjunction search in the visual search literature (see Verghese, 2001 for a review). That is, searching for a conjunction of features may depend more on precise representation of each single feature, thus possibly posing a higher demand on the representational precision as compared to searching for a single feature. Future computational and experimental research is needed to directly address this issue.

Precision and Capacity as Independent Aspects of Working Memory

Beyond informing theories about the architecture of human memory, the current results also contribute to the recent debate concerning whether WM is primarily limited by the number of items that can be simultaneously retain in the mind (i.e., capacity limit) or by the graded fidelity of these retained mental representations (i.e., precision limit, see Chapter 1 for details).

Decades of research using computational modeling (e.g., Raffone & Wolters, 2001), electrophysiology (Bastos, Loonis, Kornblith, Lundqvist, & Miller, 2018; Buschman, Siegel, Roy, & Miller, 2011), and functional imaging (e.g., Roux, Wibral, Mohr, Singer, & Uhlhaas, 2012) suggest that WM storage capacity may primarily result from a constraint in synchronizing information processing across brain regions (Luck & Vogel, 2013; E. K. Miller & Buschman, 2015). According to one computational model (Raffone & Wolters, 2001), neurons encoding different features across the brain can fire in synchronized patterns as cell assemblies. Oscillation of these neural assemblies provides a neural mechanism for sustained activity (and hence information retention) for WM. Consequently, the number of WM representations that can be simultaneously maintained may be constraint by the number of cell assemblies that can be fitted in a phase period of an oscillation with enough phase separation in between. This mechanism is essential to 1) keep different cell assemblies from firing at the same time to avoid interference, and to 2) prevent long delays between successive firings of a given cell assembly so that it does not decay too far. This model (Raffone & Wolters, 2001) has been partially supported by electrophysiological studies that found independent neural

oscillation patterns for capacity-determining mechanisms, such as retention of relevant information and suppression of distracting information (Roux & Uhlhaas, 2014; Sauseng et al., 2009). This oscillatory mechanism, however, does not provide an explanation for the qualitative aspect of WM.

The current dissertation research adds to this literature by providing converging evidence for the hippocampal mechanism underlying WM precision, which may be theoretically independent of neural oscillations (Buschman et al., 2011; Roux & Uhlhaas, 2014) and sustained neural activity (Todd & Marois, 2004; Y. Xu & Chun, 2005) in the posterior parietal and prefrontal cortices that support WM retention capacity (or effective storage capacity due to extremely large precision variability, Galeano Weber et al., 2016). That is, WM capacity and precision may be better considered as independent aspects suggested by capacity-limit theories (Cowan, 2001; Xie & Zhang, 2017a; Zhang & Luck, 2008), instead of as integrated aspects suggested by precision-limit theories (Bays & Husain, 2008), of WM representations.

Critically, the current cognitive neuroscience evidence favoring the dissociation between capacity-limit theories and precision-limit theories does not extensively rely on the model used to fit the behavioral recall data, thus void of concerns regarding which model may quantitatively yield better fits (see critics in van den Berg et al., 2014). Specifically, the critical evidence in Experiment 2 and 3 is based on within-subject comparison across precision load manipulation conditions. Due to reduced sampling resolution in the low precision load condition, fitting the data with available models would be less appropriate. This reliance on effectiveness of precision load manipulation

in Experiment 2 and 3 is mitigated by the decoding evidence from Experiment 4, such that the hippocampus not only is sensitive to task demands on WM precision but also contains precise item-specific information that can be directly decoded from the DG/CA3. Overall, using the cognitive neuroscience approach, the current dissertation provides novel evidence to more rapidly advance the understanding about the nature of WM representations.

Translational Relevance

The current dissertation research also has significant transitional implications that may shed light on commonly observed complaints about blurred memories or comprised mental clarity in a variety of health-related conditions. Although various factors such as fatigue may contribute to compromised mental clarity (e.g., Ross et al., 2013), a more fundamental neurocognitive mechanism underlying these effects of reduced mental clarity may be related to neurodevelopmental abnormality or pathological aberration in the hippocampus. For example, individuals with schizophrenia spectrum disorders often show structural and functional abnormality in the hippocampus (Dickey et al., 2007; Hickie, 2005; Keshavan et al., 2002; Modinos et al., 2009; Suzuki, 2005), which is often accompanied by reduced pattern separation function (Das, Ivleva, Wagner, Stark, & Tamminga, 2014) and worsened visual WM precision (Xie et al., 2018). It is thus possible that compromised hippocampal function associated with neurodevelopmental abnormality may account for reduced memory quality in schizophrenia spectrum disorders. Similarly, age-related declines in hippocampal functional has also been

associated with blurred memory (Leal & Yassa, 2018), which could account for reduced WM precision in older adults (Peich et al., 2013).

As such, WM precision may serve as a sensitive measure to investigate WM impairments in both clinical (e.g., schizophrenia spectrum disorders) and aging populations. The efforts to establish the relationship between aberrant memory precision and these devastating conditions, along with their neurobiological manifestations in MTL, would potentially promote the development of a Research Domain Criteria (RDoC) outcome in the cognitive domain to pave the way for improving diagnosis and defining novel targets (e.g., hippocampal metabolic compounds) for future interventions (Leal & Yassa, 2018).

Future Research Directions

As a modest step forward, the current dissertation research reveals the critical role of the hippocampus, especially its DG/CA3 subfield, in supporting precise WM representations. However, there are several outstanding questions to be addressed in future studies.

First, of primary interest, how does pattern separation computation directly contribute to WM precision? One critical assumption in the pattern separation literature is that the conversion from cortical-level population codes to hippocampal sparse codes may serve as fundamental limiting factor for precise memories. This change in coding scheme is equivalent to the conversion of an image file from a high-resolution format that uses a large number of pixels to encode the pictorial information to a more compressed format that uses a less number of pixels. As such, when information is transferred from a

perceptual representation in cortical regions to a mnemonic representation in subcortical regions (e.g., hippocampus), there may be a certain level of information loss over the conversion. This may account for the reduction of precision from perception to WM, even just after a 1-second delay between study and test (Brady et al., 2013; Cappiello & Zhang, 2016; J. M. Gold et al., 2010). However, it is difficult to directly test this mechanistic explanation of WM precision even with high-resolution fMRI (Carr et al., 2010). Future studies using computational modeling and intracranial electrophysiology will need to further examine this coding issue.

Second, how does the hippocampal pattern separation process relate to neural noise at the cortical level? As discussed in Chapter 2, the pattern separation hypothesis and neural noise hypothesis may describe processes or computations that occur at different stages of information processing, and consequently it is possible that increased hippocampal pattern separation computation may manifest as reduced cortical neural noise, leading to improved representational precision. For instance, a recent neuroimaging study showed that hippocampal signals in the DG/CA3 subfield may predict successful information encoding in the early visual cortex during statistical learning (Hindy et al., 2016). Similarly, using Granger causality analysis, Experiment 4 in the current dissertation research also shows that information from the hippocampal DG/CA3 subfield may contain information that can be predictive of that in the visual cortex during the visual WM retention interval. Nonetheless, the temporal information about the interactions between the hippocampus and sensory regions using fMRI is highly limited, even though the functional association is evaluated based on deconvolved

time serial data (Deshpande et al., 2009; Deshpande, Hu, Stilla, & Sathian, 2008; Goodyear et al., 2017). Future research with more advanced neuroimaging methods or electrophysiological recording may shed light on these potential functional dynamics.

Last but not the least, is the reduction of precision from perceptual representations to mnemonic representations a "design flaw" of human cognition, or does it serve some functional roles that entail further specification? Conventionally, variability is often considered as noise, which is detrimental for detecting a signal. However, adding noise sometimes may paradoxically boost the likelihood of detecting a signal based on the principle of stochastic resonance (Hänggi, 2002). Specifically, when the frequency of random noise corresponds to the frequency of a target signal, the noise and signal will resonate with each other, amplifying the original signal while not amplifying the random noise and hence increasing the signal-to-noise ratio (Moss, 2004). Consequently, increasing variability by introducing noise in a mental representation may in fact make the represented signal more prominent from intrinsic background neural noise. Furthermore, a less precise representation may also allow more flexible switching across different but similar representations/concepts, which is a key component of cognitive flexibility (Scott, 1962). Given the central role of WM in human cognition, how does WM precision potentially support flexible cognitive control and decision making will be an interesting future research direction.

Appendix A

Tables

Table 1. Brain areas activated monotonically to visual working memory precision load manipulation in Experiment 2

Region (MNI labels)	L/R	Brodmann area	MNI Coordinates (center-of-mass)			Cluster size	Peak *t*
			x	*y*	*z*		
Frontal							
Medial Prefrontal Gyrus	R & L	10	2	54	14	107	3.31
Parietal							
Angular Gyrus	R	39	54	-65	33	60	3.48
	L	39	-52	-61	24	163	3.21
Precuneus	L	31	-6	-54	30	77	3.81
Temporal							
Hippocampus-Amygdala Complex	L	53/54	-20	-4	-21	57	3.49

Note. Coordinates were displayed in the MNI space. L-Left; R-Right. Family-wise-error cluster correction to a significance level of .01 (two-sided), equivalent to uncorrected $p < .005$ with a clusters size >= 55.

Table 2. Results from psychophysiological interaction (PPI) analysis using the anterior and posterior hippocampi as separate seed regions in Experiment 2.

Region (MNI labels)	Polarity	L/R	Brodmann area	MNI Coordinates (center-of-mass)			Cluster size	Peak *t*
				x	*y*	*z*		
Left aHPC Seed								
Anterior Cingulate Cortex	-	L	32	-4	45	6	225	2.88
Putamen	-	R	49	31	-1	10	158	4.06
Cerebellum	-	R		17	-42	-32	161	2.42
Left pHPC Seed								
Medial Prefrontal Gyrus	+	R	9/10	38	48	31	304	4.31
	+	L	10	-38	45	32	153	2.18
Superior Parietal Lobule	+	R	7	17	-46	77	259	3.43
	+	L	7	-28	-58	71	157	2.89

Note. Coordinates were displayed in the MNI space. aHPC = anterior hippocampus; pHPC = posterior hippocampus. Family-wise-error cluster correction to a significance level of .05 (two-sided), equivalent to uncorrected $p < .05$ with a clusters size >= 150. a. Polarity refers to the direction of the PPI effects. A positive (negative) PPI result would suggest an increase (decrease) in functional connectivity between the target region and the seed region as mnemonic precision load increases.

Table 3. Brain areas containing visual working memory content in Experiment 4.

Region (MNI labels)	L/R	Brodmann area	MNI Coordinates (center-of-mass)			Cluster size	Peak *t*
			x	*y*	*z*		
Frontal							
Anterior Cingulate Cortex	L	32	-2	28	26	43	4.45
Inferior Frontal Gyrus	L	46	-44	33	17	44	5.59
Middle Frontal Gyrus	L	8	-44	13	41	40	4.61
Parietal							
Angular Gyrus	L	39	-43	-67	36	73	3.89
Precuneus	R	7	6	-48	56	73	4.07
Superior Parietal Lobule	L	7	-18	-69	59	109	12.76
	L	7	-33	-52	68	106	5.26
	R	7	21	-69	55	1314	11.57
	R	7	22	-54	70	80	4.78
Inferior Parietal Lobule	L	39	-33	-75	45	84	7.29
	R	40	47	-42	53	105	3.56
Supra Marginal Gyrus	R	40	59	-25	44	109	4.07
Temporal							
Middle Temporal Gyrus	L	39	-55	-69	21	54	4.44
	R	39	64	-49	17	116	6.37
	R	19	52	-77	13	66	5.55
Inferior Temporal Gyrus	L	20	-47	-45	-28	71	5.52
Occipital							
Calcarine Gyrus	L/R	17	5	-87	-1	2517	9.49
	L	17/18	-20	-66	17	56	6.11
	R	17	16	-63	10	344	5.82
Lingual Gyrus	L	18	-7	-63	3	74	4.22
	R	19	40	78	-17	213	7.45
	R	19	14	-43	-8	175	5.92
Middle Occipital Gyrus	L	19	-28	-85	16	167	6.91
	L	39	-29	-75	30	79	4.34
Occipital-Temporal							
Fusiform Gyrus	L	37	-25	-60	-14	315	10.80
	L	19	-40	-76	-17	58	4.29
	R	37	25	-65	-15	100	4.95

Note. Coordinates were displayed in the MNI space. L-Left; R-Right. Family-wise-error cluster correction to a significance level of .05 (one-sided), equivalent to uncorrected $p < .05$ with a clusters size >= 40.

Appendix B

Figures

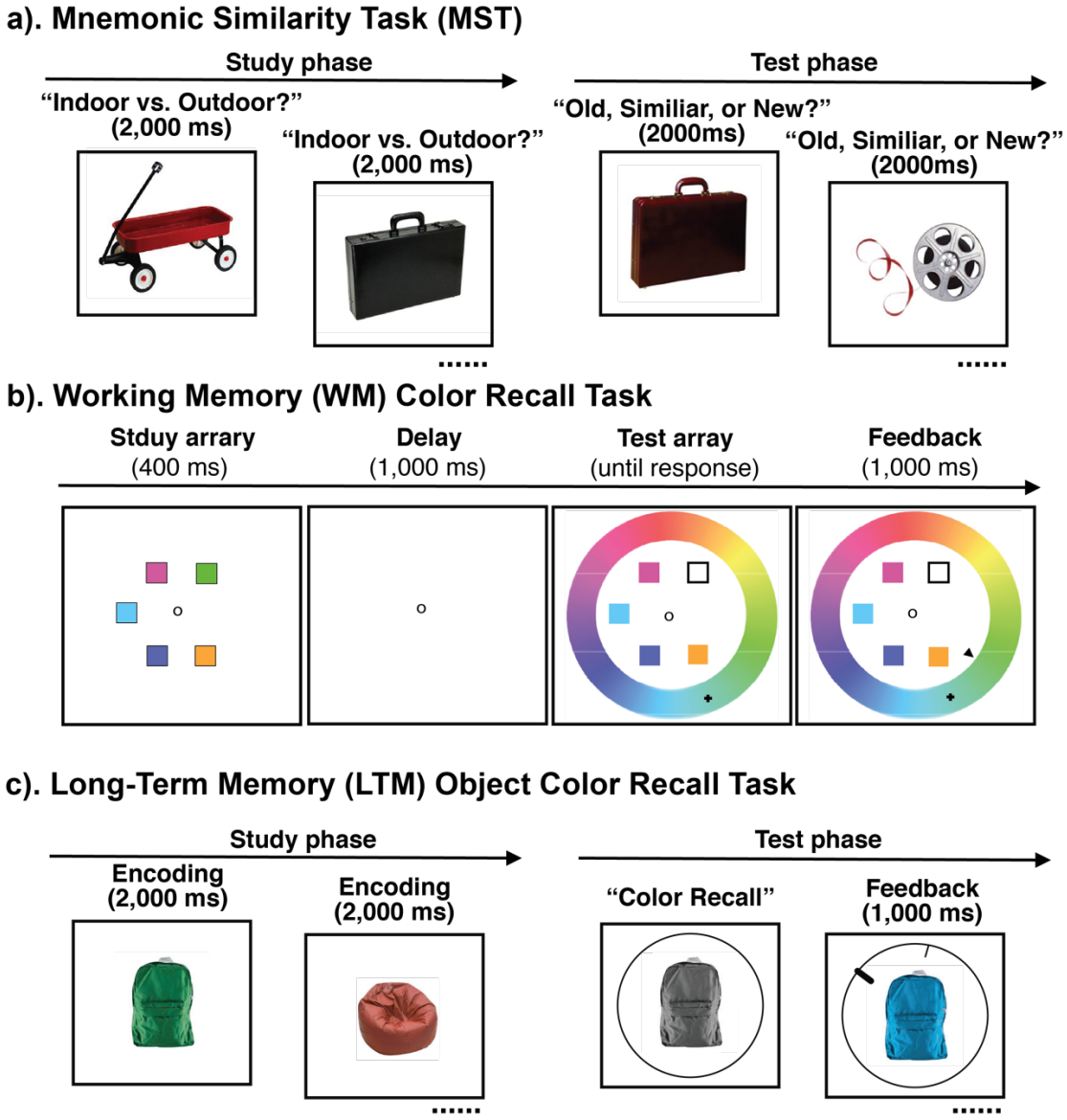

Figure 1. Behavioral paradigms used in Experiment 1. a) Mnemonic similarity task (MST); b) Working memory (WM) color recall task; c) Long-term memory (LTM) object color recall task. The mnemonic similarity task was always tested first, and the order of the WM and LTM color recall tasks was counter-balanced across subjects.

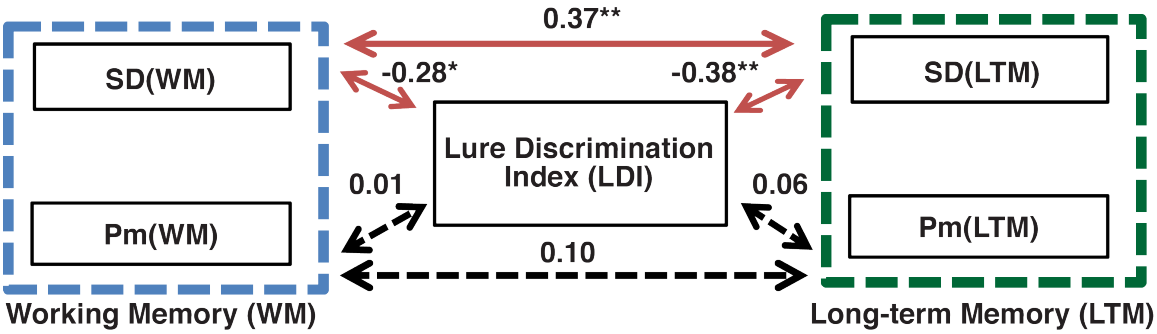

Figure 2. Associations among behavioral measures of pattern separation (i.e., lure discrimination index, LDI), mnemonic precision (SD), and the probability of successful remembering (Pm) across working memory (WM) and long-term memory (LTM) in Experiment 1. SD is an inverse estimate of mnemonic precision for retained memory representations. Pm stands for the probability of remembering. The red solid lines indicate significant associations, whereas black dashed lines indicate non-significant associations. The blue square indicates WM measures and the green square indicates LTM measures. *. $p < .05$; **. $p < .01$.

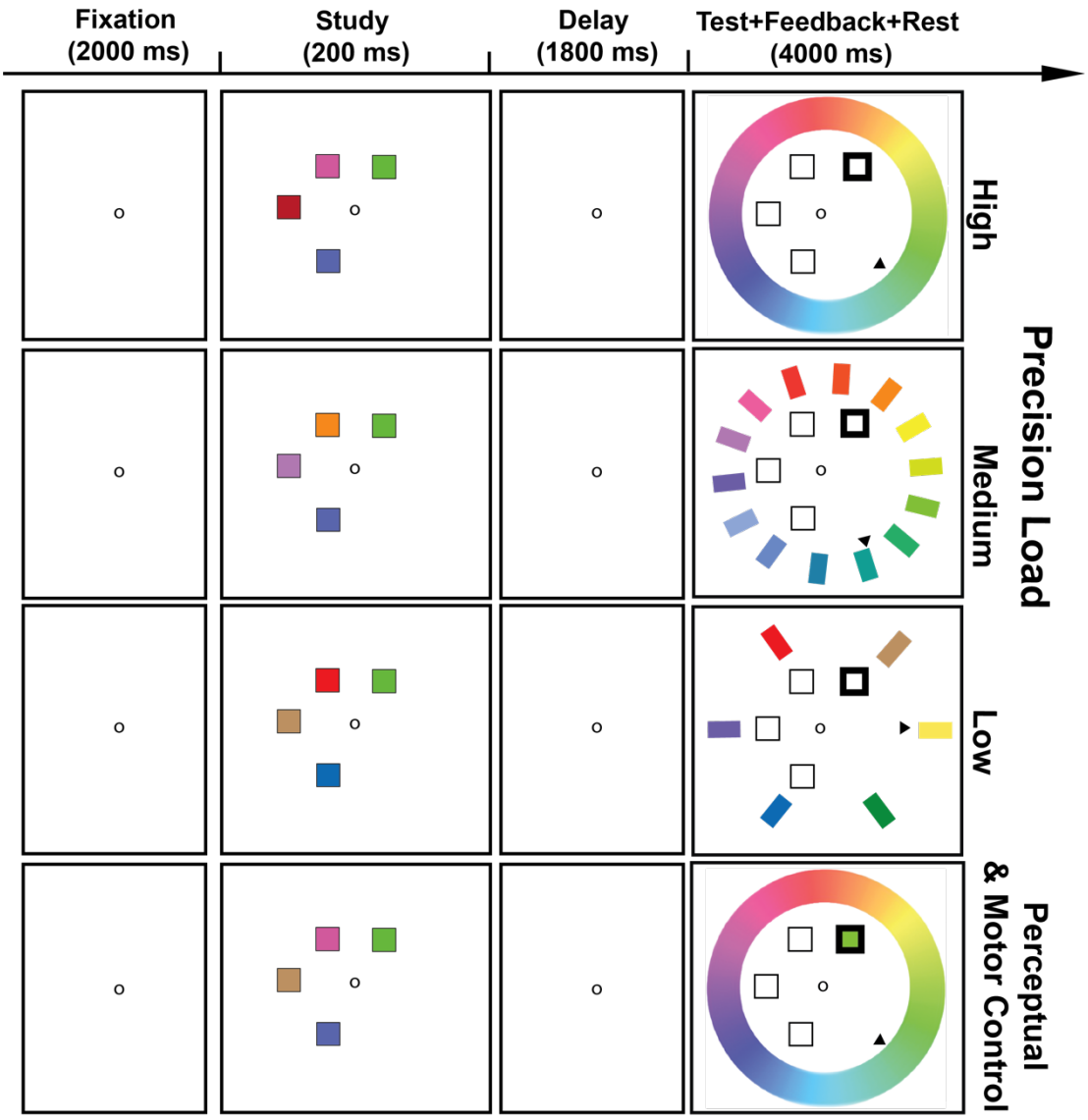

Figure 3. Behavioral paradigm used in Experiment 2 and 3. In this task, visual working memory (WM) precision was manipulated by varying the number of non-memory items in the stimulus feature space (color). Specifically, while participants remembered the same number (four) of colors in the WM conditions, these colors were randomly sampled from 180, 15, and 6 colors in the high, medium, and low precision load conditions, respectively. An additional perceptual and motor control condition (the last row) had the same perceptual and motor components but without a memory component as compared to that in the WM conditions. These different experimental conditions were blocked, with the sequence randomized by a Latin-squared design across individuals.

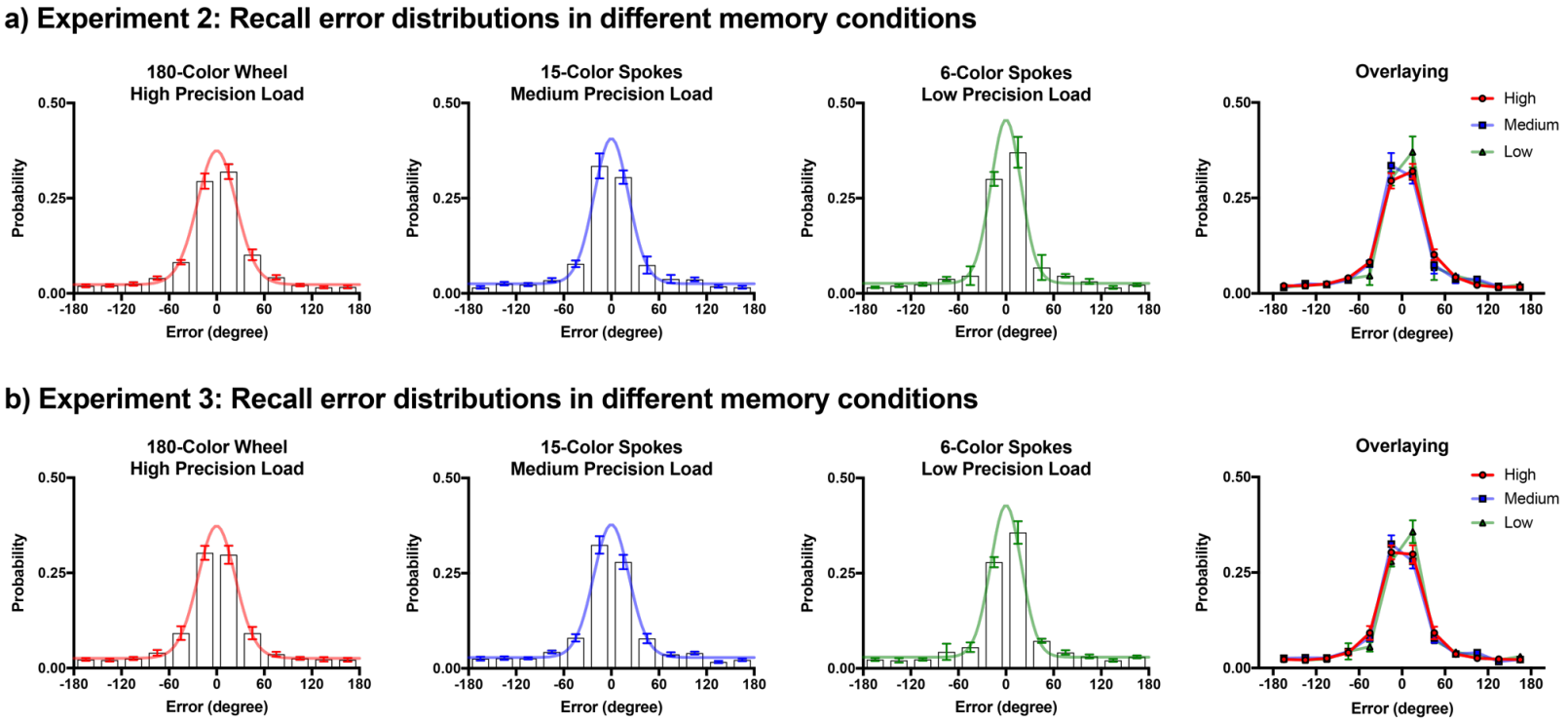

Figure 4. Recall error distributions and model fits across experimental conditions for data combining both inside scanner trials (100 trials per condition) and outside scanner trials (50 trials per condition) in Experiment 2 (a) and Experiment 3 (b). Participants seemed to retained a comparable amount of information across different precision load conditions, as indicated by comparable tails of the recall error distributions across conditions. The error bars represent standard errors of the binned data across subjects. Overall, data from Experiment 2 and Experiment 3 were highly consistently.

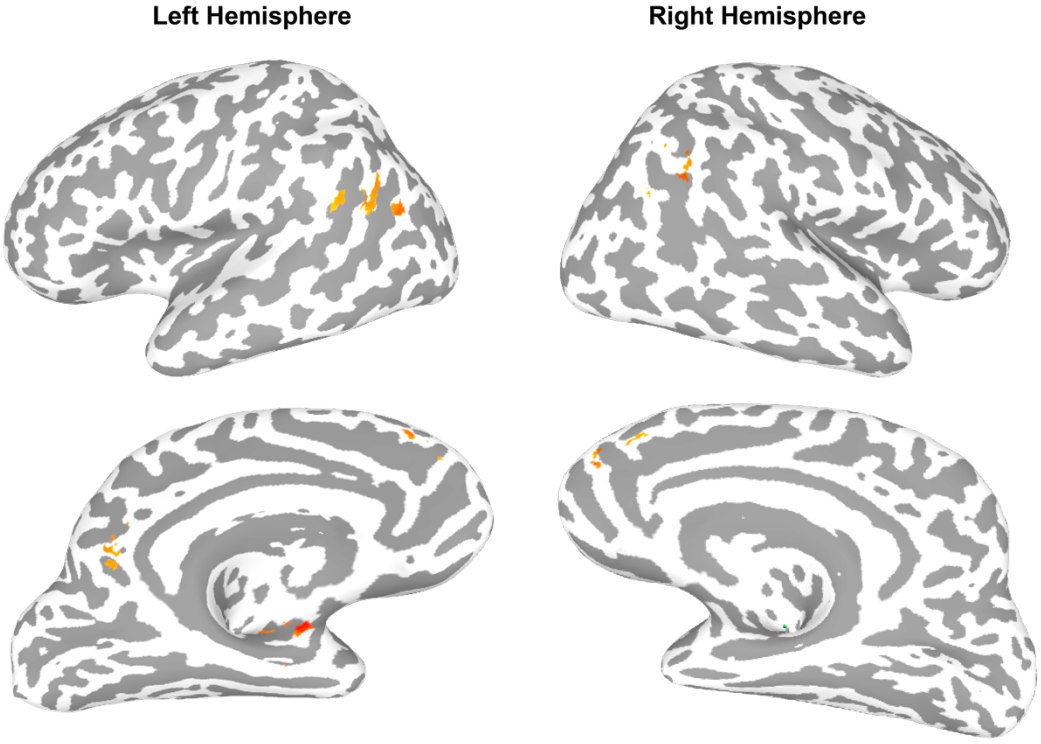

Figure 5. Brain areas activated as a function of working memory precision load manipulation in Experiment 2 (*p* corrected to .01 level, two-tailed, equivalent to uncorrected $p < .005$ with cluster size > =55 based on *3dClustSim*). Activations are displayed on the cortical surface using SUMA (https://afni.nimh.nih.gov/Suma). Coordinates of these brain regions can be found in Table 1.

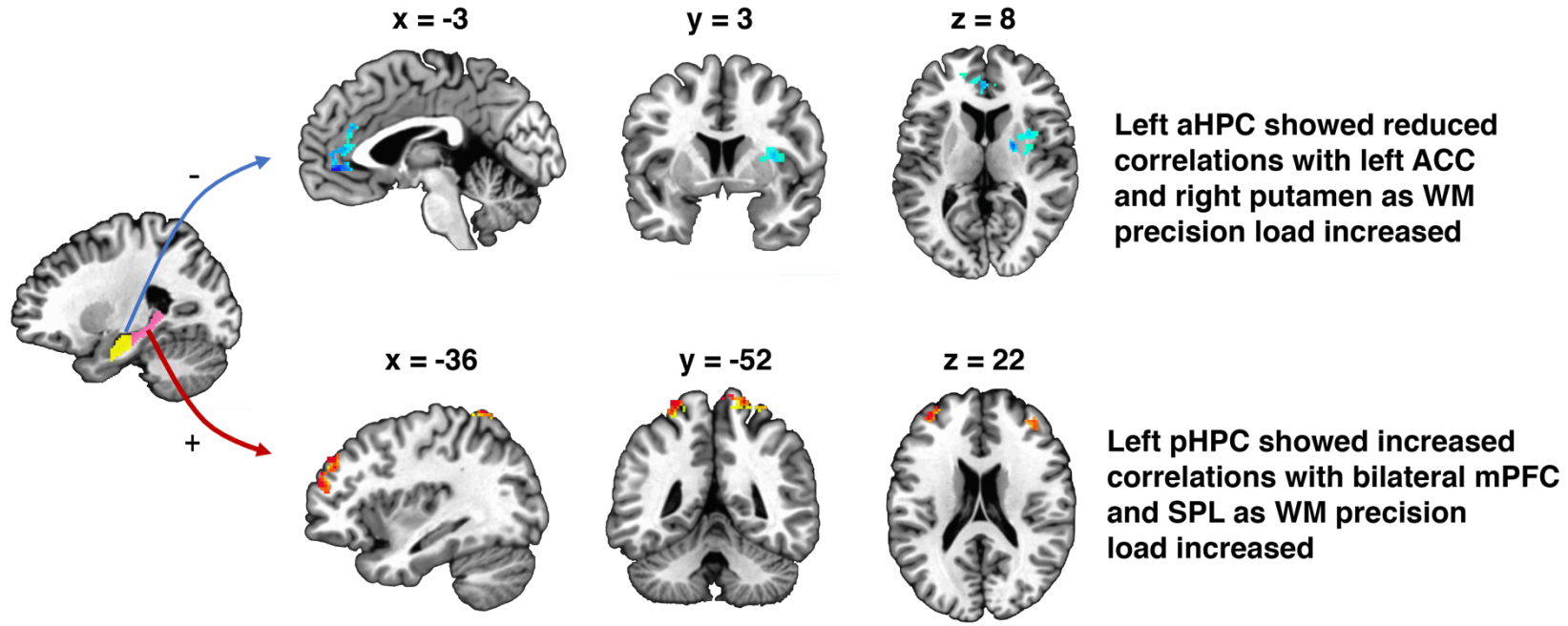

Figure 6. Psychophysiological Interaction (PPI) results obtained by using the left anterior hippocampus (left aHPC, masked in yellow) and the left posterior hippocampus (left pHPC, masked in pink) as seed regions. The left aHPC decoupled with the left ACC and right putamen, while the left HPC coupled with bilateral mPFC (middle prefrontal cortex) and SPL (Superior Parietal Lobule), as WM (working memory) precision load increased. Brain areas were considered as significance at .05 level with uncorrected $p < .05$ and a cluster size >= 150. Coordinates of these brain regions can be found in Table 2. Coordinates were displayed in the MNI space in this figure.

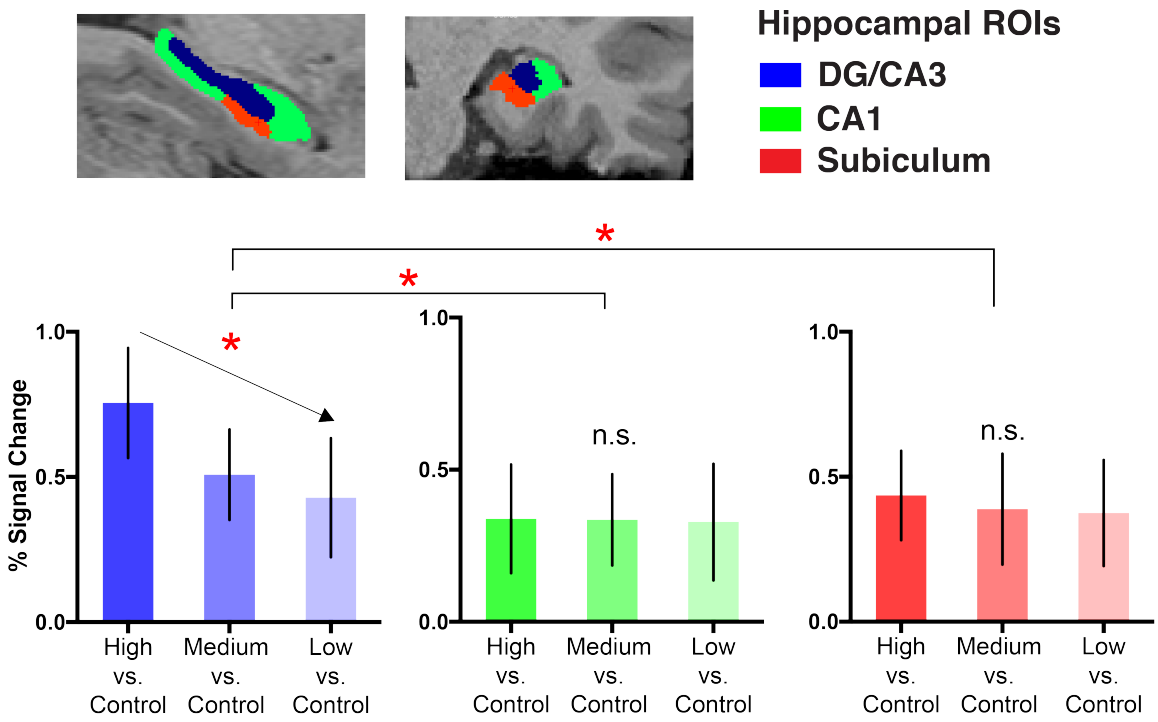

Figure 7. Activation in the DG/CA3 was monotonically modulated by precision load manipulation in Experiment 3. This monotonically-decreasing pattern, however, was not significant in the CA1 and subiculum. There were also significant interaction effects between DG/CA3 versus CA1 and between DG/CA3 versus subiculum, in terms of the linear contrast across experimental conditions. *. $p < .05$

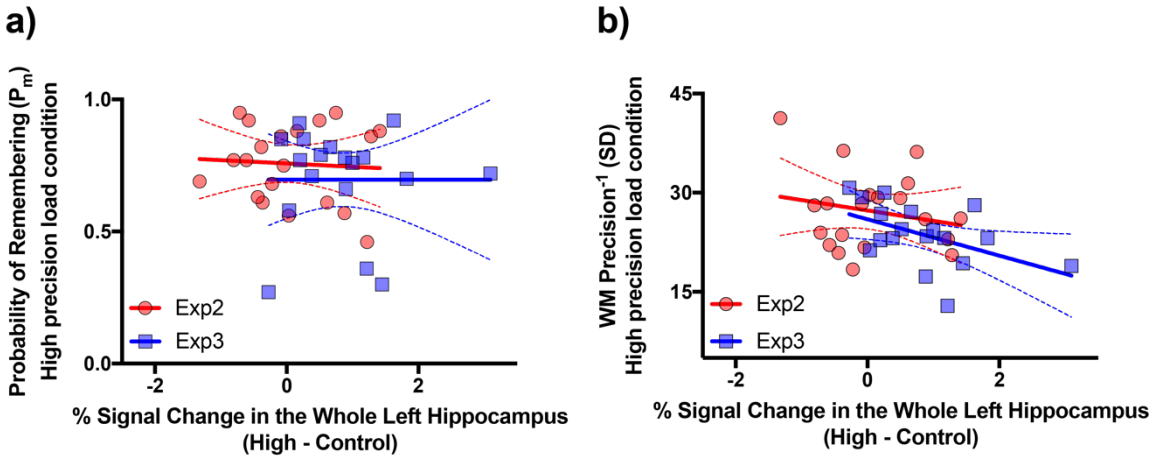

Figure 8. Correlations between hippocampal activity and visual working memory probability of remembering, Pm (a) and precision, SD (b) in the high precision-load condition across Experiment 2 and 3. Hippocampal activity in the high-precision load condition is calculated relative to that in the perceptual/motor control condition. The red dots represent data from Experiment 2 and the blue squares represent data from Experiment 3. The linear regression fits with 95% confidence intervals are calculated and plotted separately for each data. The results were meta-analytically combined for inference (see General Discussion in Chapter 4 for details).

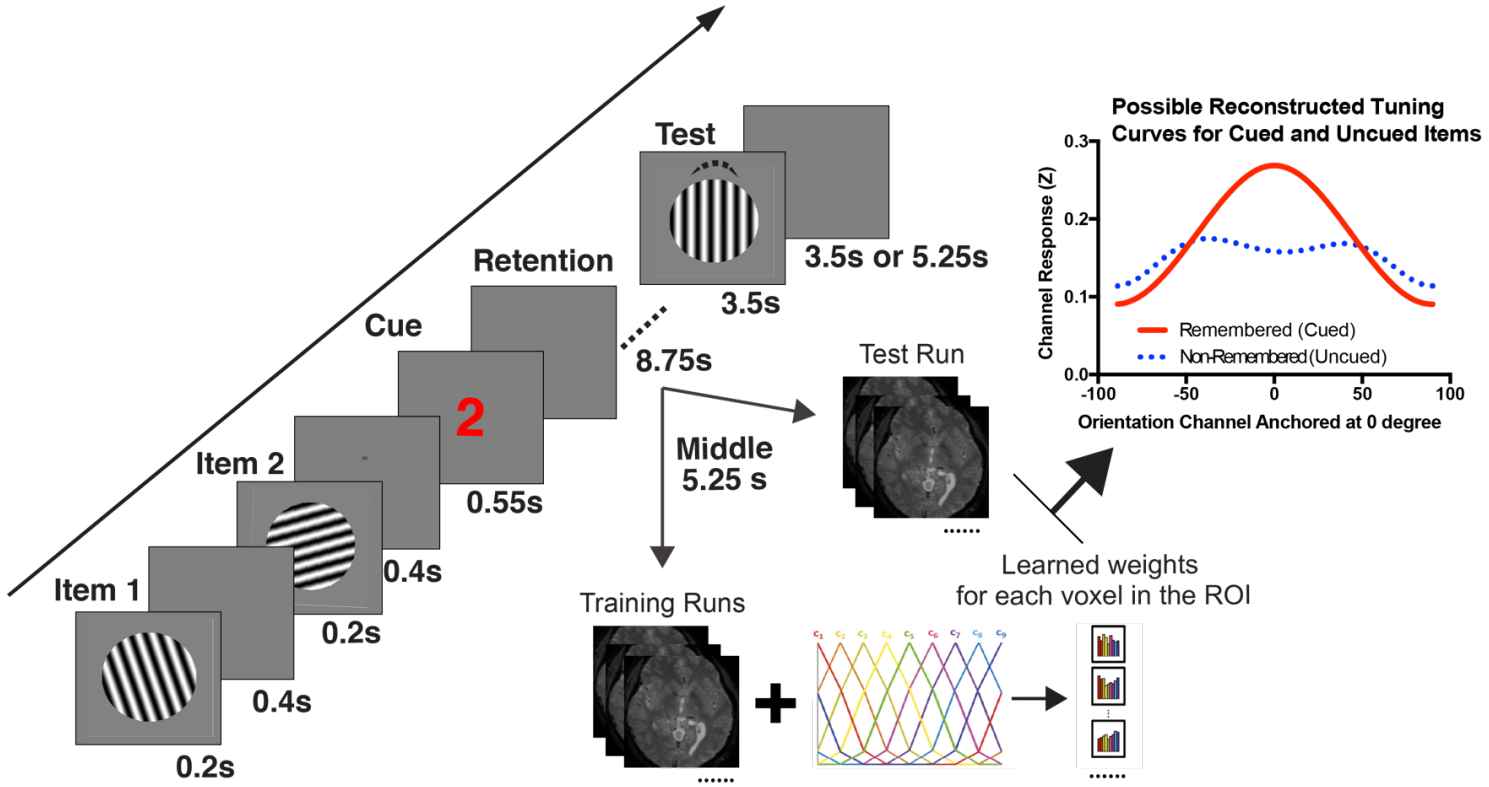

Figure 9. Paradigm and the Inverted Encoding Model analysis in Experiment 4. On each trial (left side), participants memorize the orientation of two sequentially presented gratings and then only maintain one (remembered) while ignoring the other (non-remembered), based on a number cue presented afterwards. After a short delay, participants report the to-be-remembered orientation from memory by reproducing its orientation on a test grating using the method of adjustment. In a leave-one-run-out cross-validation procedure, fMRI signals in training runs during visual working memory retention interval will be modeled as a weighted sum of 9 hypothetical orientation channels. These trained weights will be applied to an independent test run, such that orientation channels can be reconstructed. If a region contains decodable item-specific information, it is expected that the reconstruction of response channels should peak at 0, after centering these channels at 0.

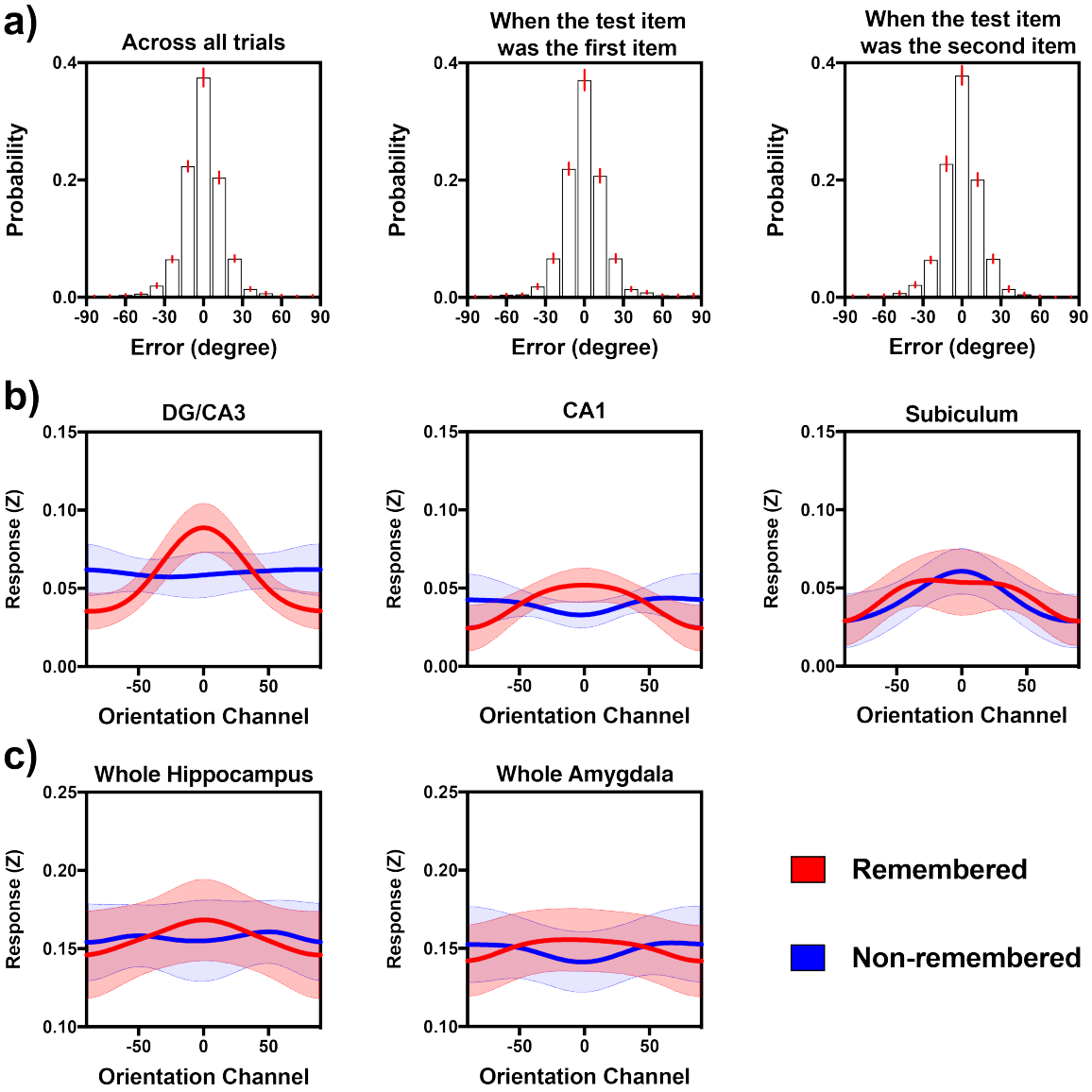

Figure 10. Behavioral and region-of-interest (ROI) analysis results in Experiment 4. (a) Participants recall error distributions across all trials, when the test item was the first item, and when the test item was the second item; (b) Reconstructions of the remembered and non-remembered orientations in each hippocampal ROI; (c) Reconstructions of the remembered and non-remembered orientations in the whole hippocampus and the amygdala. Data were averaged across samples obtained in the last 3 TRs following the onset of the sample display before modeling.

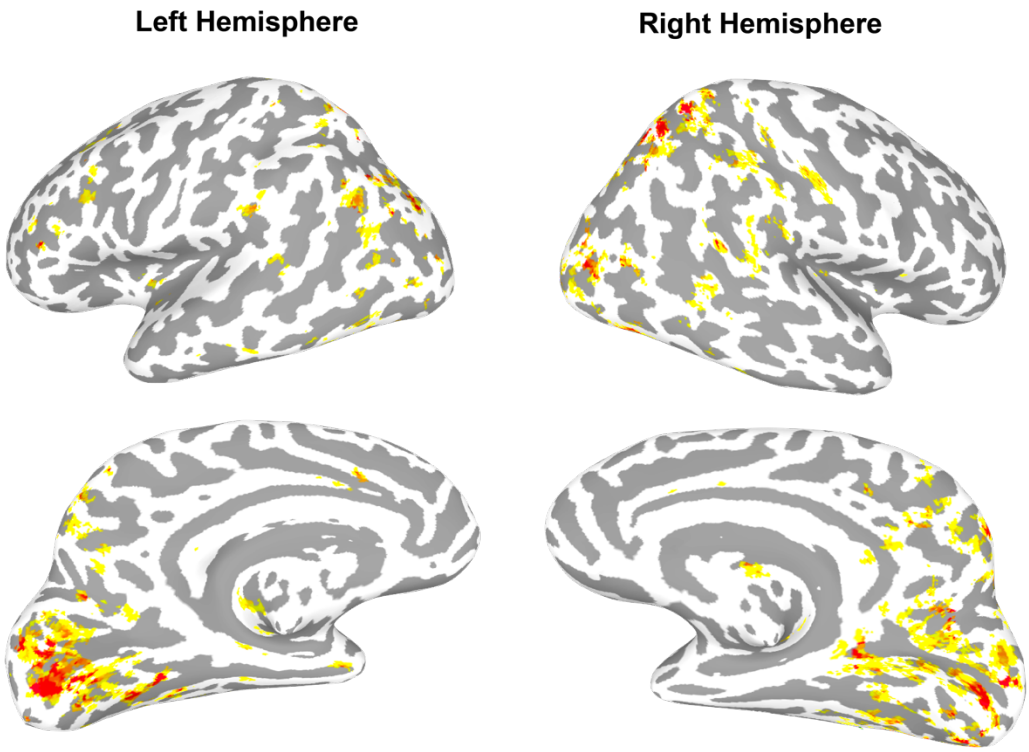

Figure 11. Brain areas that contained decodable visual working memory content during the delay period in Experiment 4 based on a whole-brain searchlight analysis (*p* corrected to .05 level, one-tailed, equivalent to uncorrected $p < .05$ with cluster size >= 40 based on *3dClustSim*). Activations are displayed on the cortical surface using SUMA (https://afni.nimh.nih.gov/Suma). Coordinates of these brain regions can be found in Table 3.

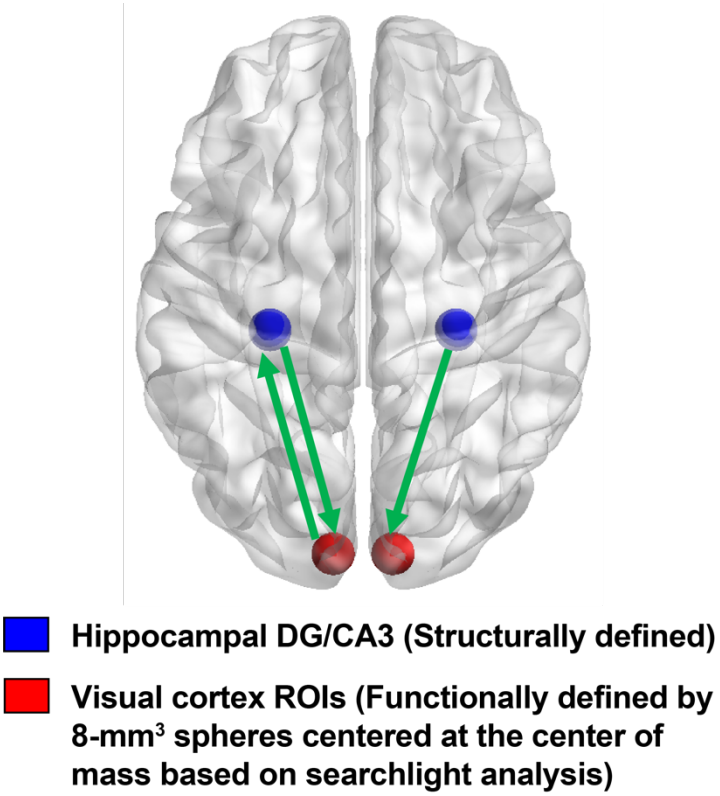

Figure 12. Granger causal relationship during the last 3TRs of the visual working memory delay period between hippocampal DG/CA3 and visual cortex ROIs extracted from the searchlight analysis. The arrows indicate directionality. The green solid line indicates a significant association after Bonferroni correction (corrected $p < .05$).

References

Addante, R. J. (2015). A critical role of the human hippocampus in an electrophysiological measure of implicit memory. *NeuroImage*, *109*, 515–528.

Aimone, J. B., Deng, W., & Gage, F. H. (2011). Resolving new memories: A critical look at the dentate gyrus, adult neurogenesis, and pattern separation. *Neuron*, *70*(4), 589–596.

Alvarez, G. A., & Cavanagh, P. (2004). The capacity of visual short-term memory is set both by visual information load and by number of objects. *Psychological Science*, *15*(2), 106–111.

Atkinson, R. C., & Shiffrin, R. M. (1968). Human memory: A proposed system and its control processes. *Psychology of Learning and Motivation*, *2*, 89–195.

Avants, B. B., Tustison, N. J., Stauffer, M., Song, G., Wu, B., & Gee, J. C. (2014). The Insight ToolKit image registration framework. *Frontiers in Neuroinformatics*, *8*(52), 773.

Avants, B. B., Yushkevich, P., Pluta, J., Minkoff, D., Korczykowski, M., Detre, J., & Gee, J. C. (2010). The optimal template effect in hippocampus studies of diseased populations. *NeuroImage*, *49*(3), 2457–2466.

Avants, B., Duda, J. T., Kim, J., Zhang, H., Pluta, J., Gee, J. C., & Whyte, J. (2008). Multivariate analysis of structural and diffusion imaging in traumatic brain injury. *Academic Radiology*, *15*(11), 1360–1375.

Axmacher, N., Mormann, F., Fernández, G., Cohen, M. X., Elger, C. E., & Fell, J. (2007). Sustained neural activity patterns during working memory in the human medial temporal lobe. *Journal of Neuroscience*, *27*(29), 7807–7816.

Baddeley, A. (2012). Working memory: Theories, models, and controversies. *Annual Review of Psychology*, *63*, 1–29.

Baddeley, A. D., & Hitch, G. (1974). Working memory. *Psychology of Learning and Motivation*, *8*, 47–89.

Baddeley, A. D., & Warrington, E. K. (1970). Amnesia and the distinction between long- and short-term memory. *Journal of Verbal Learning and Verbal Behavior*, *9*(2), 176–189.

Bakker, A., Kirwan, C. B., Miller, M., & Stark, C. E. L. (2008). Pattern separation in the human hippocampal CA3 and dentate gyrus. *Science*, *319*(5870), 1640–1642.

Banta Lavenex, P., Boujon, V., Ndarugendamwo, A., & Lavenex, P. (2015). Human short-term spatial memory: precision predicts capacity. *Cognitive Psychology*, *77*, 1–19.

Barense, M. D., Gaffan, D., & Graham, K. S. (2007). The human medial temporal lobe processes online representations of complex objects. *Neuropsychologia*, *45*(13), 2963–2974.

Bastos, A. M., Loonis, R., Kornblith, S., Lundqvist, M., & Miller, E. K. (2018). Laminar recordings in frontal cortex suggest distinct layers for maintenance and control of working memory. *Proceedings of the National Academy of Sciences of the United States of American*, *63*, 201710323–7.

Bays, P. M. (2014). Noise in neural populations accounts for errors in working memory. *Journal of Neuroscience*, *34*(10), 3632–3645.

Bays, P. M. (2015). Spikes not slots: noise in neural populations limits working memory. *Trends in Cognitive Sciences*, *19*(8), 431–438.

Bays, P. M., & Husain, M. (2008). Dynamic shifts of limited working memory resources in human vision. *Science*, *321*(5890), 851–854.

Bettencourt, K. C., & Xu, Y. (2015). Decoding the content of visual short-term memory under distraction in occipital and parietal areas. *Nature Neuroscience*, *19*(1), 150–157.

Bickle, J. (1998). Psychoneural Reduction. Cambridge, Massachusetts: MIT Press.

Brady, T. F., Konkle, T., Alvarez, G. A., & Oliva, A. (2008). Visual long-term memory has a massive storage capacity for object details. *Proceedings of the National Academy of Sciences of the United States of America*, *105*(38), 14325–14329.

Brady, T. F., Konkle, T., Gill, J., Oliva, A., & Alvarez, G. A. (2013). Visual long-term memory has the same limit on fidelity as visual working memory. *Psychological Science*, *24*(6), 981–990.

Buschman, T. J., Siegel, M., Roy, J. E., & Miller, E. K. (2011). Neural substrates of cognitive capacity limitations. *Proceedings of the National Academy of Sciences of the United States of America*, *108*(27), 11252–11255.

Cappiello, M., & Zhang, W. (2016). A dual-trace model for visual sensory memory. *Journal of Experimental Psychology: Human Perception and Performance*, *42*(11), 1903–1922.

Carr, V. A., Rissman, J., & Wagner, A. D. (2010). Imaging the human medial temporal lobe with high-resolution fMRI. *Neuron*, *65*(3), 298–308.

Chang, M. H., Armstrong, K. M., & Moore, T. (2012). Dissociation of response variability from firing rate effects in frontal eye field neurons during visual stimulation, working memory, and attention. *Journal of Neuroscience*, *32*(6), 2204–2216.

Christophel, T. B., Klink, P. C., Spitzer, B., Roelfsema, P. R., & Haynes, J.-D. (2017). The distributed nature of working memory. *Trends in Cognitive Sciences*, *21*(2), 111–124.

Cisler, J. M., Bush, K., & Steele, J. S. (2014). A comparison of statistical methods for detecting context-modulated functional connectivity in fMRI. *NeuroImage*, *84*(C), 1042–1052.

Clelland, C. D., Choi, M., Romberg, C., Clemenson, G. D., Fragniere, A., Tyers, P., et al. (2009). A functional role for adult hippocampal neurogenesis in spatial pattern separation. *Science*, *325*(5937), 210–213.

Cohen, M. A., Konkle, T., Rhee, J. Y., Nakayama, K., & Alvarez, G. A. (2014). Processing multiple visual objects is limited by overlap in neural channels. *Proceedings of the National Academy of Sciences of the United States of America*, *111*(24), 8955–8960.

Conway, A. R. A., Kane, M. J., & Engle, R. W. (2003). Working memory capacity and its relation to general intelligence. *Trends in Cognitive Sciences*, *7*(12), 547–552.

Conway, M. A. (1991). In defense of everyday memory. *American Psychologist*, *46*(1), 19–26.

Cooper, H., & Patall, E. A. (2009). The relative benefits of meta-analysis conducted with individual participant data versus aggregated data. *Psychological Methods*, *14*(2), 165–176.

Cornelissen, F. W., & Greenlee, M. W. (2000). Visual memory for random block patterns defined by luminance and color contrast. *Vision Research*, *40*(3), 287–299.

Courtney, S. M., Ungerleider, L. G., Keil, K., & Haxby, J. V. (1997). Transient and sustained activity in a distributed neural system for human working memory. *Nature*, *386*(6625), 608–611.

Cowan, N. (2001). The magical number 4 in short-term memory: A reconsideration of mental storage capacity. *Behavioral and Brain Sciences*, *24*(1), 87–185.

Cox, R. W. (1996). AFNI: Software for analysis and visualization of functional magnetic resonance neuroimages. *Computers and Biomedical Research, an International Journal*, *29*(3), 162–173.

Das, T., Ivleva, E. I., Wagner, A. D., Stark, C. E. L., & Tamminga, C. A. (2014). Loss of pattern separation performance in schizophrenia suggests dentate gyrus dysfunction. *Schizophrenia Research*, *159*(1), 193–197.

Degonda, N., Mondadori, C. R. A., Bosshardt, S., Schmidt, C. F., Boesiger, P., Nitsch, R. M., et al. (2005). Implicit Associative Learning Engages the Hippocampus and Interacts with Explicit Associative Learning. *Neuron*, *46*(3), 505–520.

Deng, W., Aimone, J. B., & Gage, F. H. (2010). New neurons and new memories: How does adult hippocampal neurogenesis affect learning and memory? *Nature Reviews Neuroscience*, *11*(5), 1–12.

Deshpande, G., Hu, X., Stilla, R., & Sathian, K. (2008). Effective connectivity during haptic perception: A study using Granger causality analysis of functional magnetic resonance imaging data. *NeuroImage*, *40*(4), 1807–1814.

Deshpande, G., LaConte, S., James, G. A., Peltier, S., & Hu, X. (2009). Multivariate Granger causality analysis of fMRI data. *Human Brain Mapping*, *30*(4), 1361–1373.

Di Martino, A., Scheres, A., Margulies, D. S., Kelly, A. M. C., Uddin, L. Q., Shehzad, Z., et al. (2008). Functional Connectivity of Human Striatum: A Resting State fMRI Study. *Cerebral Cortex*, *18*(12), 2735–2747.

Diana, R. A., Yonelinas, A. P., & Ranganath, C. (2007). Imaging recollection and familiarity in the medial temporal lobe: A three-component model. *Trends in Cognitive Sciences*, *11*(9), 379–386.

Dickey, C. C., McCarley, R. W., Xu, M. L., Seidman, L. J., Voglmaier, M. M., Niznikiewicz, M. A., et al. (2007). MRI abnormalities of the hippocampus and cavum septi pellucidi in females with schizotypal personality disorder. *Schizophrenia Research*, *89*(1-3), 49–58.

Donkin, C., Nosofsky, R., Gold, J., & Shiffrin, R. (2015). Verbal labeling, gradual decay, and sudden death in visual short-term memory. *Psychonomic Bulletin & Review*, *22*(1), 170–178.

Eichenbaum, H. (2014). Time cells in the hippocampus: a new dimension for mapping memories. *Nature Reviews Neuroscience*, *15*(11), 732–744.

Eichenbaum, H., & Cohen, N. J. (2014). Can we reconcile the declarative memory and spatial navigation views on hippocampal function? *Neuron*, *83*(4), 764–770.

Eichenbaum, H., Yonelinas, A. P., & Ranganath, C. (2007). The medial temporal lobe and recognition memory. *Annual Review of Neuroscience*, *30*(1), 123–152.

Emrich, S. M., Riggall, A. C., LaRocque, J. J., & Postle, B. R. (2013). Distributed patterns of activity in sensory cortex reflect the precision of multiple items maintained in visual short-term memory. *Journal of Neuroscience*, *33*(15), 6516–

Eriksson, J., Vogel, E. K., Lansner, A., Bergström, F., & Nyberg, L. (2015). Neurocognitive architecture of working memory. *Neuron*, *88*(1), 33–46.

Ester, E. F., Anderson, D. E., Serences, J. T., & Awh, E. (2013). A neural measure of precision in visual working memory. *Journal of Cognitive Neuroscience*, *25*(5), 754–761.

Ester, E. F., Sprague, T. C., & Serences, J. T. (2015). Parietal and frontal cortex encode stimulus-specific mnemonic representations during visual working memory. *Neuron*, *87*(4), 893–905.

Feng, C., Deshpande, G., Liu, C., Gu, R., Luo, Y.-J., & Krueger, F. (2015). Diffusion of responsibility attenuates altruistic punishment: A functional magnetic resonance imaging effective connectivity study. *Human Brain Mapping*, *37*(2), 663–677.

FitzGerald, T. H. B., Moran, R. J., Friston, K. J., & Dolan, R. J. (2015). Precision and neuronal dynamics in the human posterior parietal cortex during evidence accumulation. *NeuroImage*, *107*(C), 219–228.

Fortin, N. J., Wright, S. P., & Eichenbaum, H. (2004). Recollection-like memory retrieval in rats is dependent on the hippocampus. *Nature*, *431*(7005), 188–191.

Frankland, P. W., & Bontempi, B. (2005). The organization of recent and remote memories. *Nature Reviews Neuroscience*, *6*(2), 119–130.

Friston, K. J. (2011). Functional and Effective Connectivity: A Review. *Brain Connectivity*, *1*(1), 13–36.

Fuster, J. M. (2009). Cortex and memory: Emergence of a new paradigm. *Journal of Cognitive Neuroscience*, *21*(11), 2047–2072.

Fuster, J. M., & Alexander, G. E. (1971). Neuron activity related to short-term memory. *Science*, *173*(3997), 652–654.

Galeano Weber, E. M., Peters, B., Hahn, T., Bledowski, C., & Fiebach, C. J. (2016). Superior intraparietal sulcus controls the variability of visual working memory precision. *Journal of Neuroscience*, *36*(20), 5623–5635.

Gilbert, P. E., & Kesner, R. P. (2006). The role of the dorsal CA3 hippocampal subregion in spatial working memory and pattern separation. *Behavioural Brain Research*, *169*(1), 142–149.

Gilbert, P. E., Kesner, R. P., & Lee, I. (2001). Dissociating hippocampal subregions: A double dissociation between dentate gyrus and CA1. *Hippocampus*, *11*(6), 626–636.

Glover, G. H. (1999). Deconvolution of impulse response in event-related BOLD fMRI. *NeuroImage*, *9*(4), 416–429.

Goh, J. X., Hall, J. A., & Rosenthal, R. (2016). Mini Meta-Analysis of Your Own Studies: Some Arguments on Why and a Primer on How. *Social and Personality Psychology Compass*, *10*(10), 535–549.

Gold, J. M., Hahn, B., Zhang, W., Robinson, B. M., Kappenman, E. S., Beck, V. M., & Luck, S. J. (2010). Reduced capacity but spared precision and maintenance of working memory representations in schizophrenia. *Archives of General Psychiatry*, *67*(6), 570–577.

Goldman-Rakic, P. (1995). Cellular basis of working memory. *Neuron*, *14*(3), 477–485.

Goodyear, K., Parasuraman, R., Chernyak, S., de Visser, E., Madhavan, P., Deshpande, G., & Krueger, F. (2017). An fMRI and effective connectivity study investigating miss errors during advice utilization from human and machine agents. *Social Neuroscience*, *12*(5), 570–581.

Graham, K. S., Barense, M. D., & Lee, A. C. H. (2010). Going beyond LTM in the MTL: A synthesis of neuropsychological and neuroimaging findings on the role of the medial temporal lobe in memory and perception. *Neuropsychologia*, *48*(4), 831–853.

Granger, C. W. J. (1969). Investigating Causal Relations by Econometric Models and Cross-spectral Methods. *Econometrica*, *37*(3), 424–16.

Gruneberg, M. M., Morris, P. E., & Sykes, R. N. (1991). The obituary on everyday memory and its practical applications is premature. *American Psychologist*, *46*(1), 74–76.

Hannula, D. E., Tranel, D., & Cohen, N. J. (2006). The long and the short of it: Relational memory impairments in amnesia, even at short lags. *Journal of Neuroscience*, *26*(32), 8352–8359.

Harrison, S. A., & Tong, F. (2009). Decoding reveals the contents of visual working memory in early visual areas. *Nature*, *458*(7238), 632–635.

Hartley, T., Bird, C. M., Chan, D., Cipolotti, L., Husain, M., Vargha-Khadem, F., & Burgess, N. (2007). The hippocampus is required for short-term topographical memory in humans. *Hippocampus*, *17*(1), 34–48.

Haynes, J.-D. (2015). A Primer on Pattern-Based Approaches to fMRI: Principles, Pitfalls, and Perspectives. *Neuron*, *87*(2), 257–270.

Hänggi, P. (2002). Stochastic resonance in biology: How noise can enhance detection of weak signals and help improve biological information processing. *Chemphyschem*, *3*(3), 285–290.

Hickie, I. (2005). Reduced hippocampal volumes and memory loss in patients with early- and late-onset depression. *The British Journal of Psychiatry*, *186*(3), 197–202.

Hillyard, S. A., & Anllo-Vento, L. (1998). Event-related brain potentials in the study of visual selective attention. *Proceedings of the National Academy of Sciences of the United States of American*, *95*(3), 781–787.

Hindy, N. C., Ng, F. Y., & Turk-Browne, N. B. (2016). Linking pattern completion in the hippocampus to predictive coding in visual cortex. *Nature Neuroscience*, *19*(5), 665–667.

Irfanoglu, M. O., Modi, P., Nayak, A., Hutchinson, E. B., Sarlls, J., & Pierpaoli, C. (2015). DR-BUDDI (Diffeomorphic Registration for Blip-Up blip-Down Diffusion Imaging) method for correcting echo planar imaging distortions. *NeuroImage*, *106*, 284–299.

Jeneson, A., & Squire, L. R. (2012). Working memory, long-term memory, and medial temporal lobe function. *Learning & Memory*, *19*(1), 15–25.

Jeneson, A., Mauldin, K. N., & Squire, L. R. (2010). Intact working memory for relational information after medial temporal lobe damage. *Journal of Neuroscience*, *30*(41), 13624–13629.

Jeneson, A., Mauldin, K. N., Hopkins, R. O., & Squire, L. R. (2011). The role of the hippocampus in retaining relational information across short delays: the importance of memory load. *Learning & Memory*, *18*(5), 301–305.

Jeneson, A., Wixted, J. T., Hopkins, R. O., & Squire, L. R. (2012). Visual working memory capacity and the medial temporal lobe. *Journal of Neuroscience*, *32*(10), 3584–3589.

Johnston, S. T., Shtrahman, M., Parylak, S., Gonçalves, J. T., & Gage, F. H. (2016). Paradox of pattern separation and adult neurogenesis: A dual role for new neurons balancing memory resolution and robustness. *Neurobiology of Learning and Memory*, *129*(C), 60–68.

Jonides, J., Lewis, R. L., Nee, D. E., Lustig, C. A., Berman, M. G., & Moore, K. S. (2008). The mind and brain of short-term memory. *Annual Review of Psychology*, *59*, 193–224.

Kamiński, J., Sullivan, S., Chung, J. M., Ross, I. B., Mamelak, A. N., & Rutishauser, U. (2017). Persistently active neurons in human medial frontal and medial temporal lobe support working memory. *Nature Neuroscience*, *20*(4), 590-601.

Kane, M. J., Poole, B. J., Tuholski, S. W., & Engle, R. W. (2006). Working memory capacity and the top-down control of visual search: Exploring the boundaries of "executive attention". *Journal of Experimental Psychology: Learning, Memory, and Cognition*, *32*(4), 749–777.

Keshavan, M. S., Dick, E., Mankowski, I., Harenski, K., Montrose, D. M., Diwadkar, V., & DeBellis, M. (2002). Decreased left amygdala and hippocampal volumes in young offspring at risk for schizophrenia. *Schizophrenia Research*, *58*(2-3), 173–183.

Kirwan, C. B., Hartshorn, A., Stark, S. M., Goodrich-Hunsaker, N. J., Hopkins, R. O., & Stark, C. E. L. (2012). Pattern separation deficits following damage to the hippocampus. *Neuropsychologia*, *50*(10), 2408–2414.

Knowlton, B. J., Mangels, J. A., & Squire, L. R. (1996). A neostriatal habit learning system in humans. *Science*, *273*(5280), 1399–1402.

Koriat, A., & Goldsmith, M. (1994). Memory in naturalistic and laboratory contexts: distinguishing the accuracy-oriented and quantity-oriented approaches to memory assessment. *Journal of Experimental Psychology: General*, *123*(3), 297–315.

Koriat, A., & Goldsmith, M. (1996). Memory metaphors and the real-life/laboratory controversy: Correspondence versus storehouse conceptions of memory. *Behavioral and Brain Sciences*, *19*(02), 167–188.

Koriat, A., Goldsmith, M., & Pansky, A. (2000). Toward a psychology of memory accuracy. *Annual Review of Psychology*, *51*(1), 481–537.

Koyluoglu, O. O., Pertzov, Y., Manohar, S., Husain, M., & Fiete, I. R. (2017). Fundamental bound on the persistence and capacity of short-term memory stored as graded persistent activity. *eLife*, *6*, e22225.

Kurzban, R., Duckworth, A., Kable, J. W., & Myers, J. (2013). An opportunity cost model of subjective effort and task performance. *Behavioral and Brain Sciences*, *36*(06), 661–679.

Lacy, J. W., Yassa, M. A., Stark, S. M., Muftuler, L. T., & Stark, C. E. L. (2011). Distinct pattern separation related transfer functions in human CA3/dentate and CA1 revealed using high-resolution fMRI and variable mnemonic similarity. *Learning & Memory*, *18*(1), 15–18.

Lagarias, J. C., Reeds, J. A., Wright, M. H., & Wright, P. E. (1998). Convergence properties of the Nelder-Mead simplex method in low dimensions. *SIAM Journal on Optimization*, *9*(1), 112–147.

Leal, S. L., & Yassa, M. A. (2018). Integrating new findings and examining clinical applications of pattern separation. *Nature Neuroscience*, 1–12.

Lee, A., Yeung, L.-K., & Barense, M. D. (2012). The hippocampus and visual perception. *Frontiers in Human Neuroscience*, *6*, 91.

Lee, A., Barense, M., & Graham, K. (2005). The contribution of the human medial temporal lobe to perception: Bridging the gap between animal and human studies. *The Quarterly Journal of Experimental Psychology: Section B*, *58*(3-4), 300–325.

Lee, B., & Harris, J. (1996). Contrast transfer characteristics of visual short-term memory. *Vision Research*, *36*(14), 2159–2166.

Lewis-Peacock, J. A., & Postle, B. R. (2008). Temporary activation of long-term memory supports working memory. *Journal of Neuroscience*, *28*(35), 8765–8771.

Li, M., Long, C., & Yang, L. (2015). Hippocampal-prefrontal circuit and disrupted functional connectivity in psychiatric and neurodegenerative disorders. *BioMed Research International*, *2015*, 810548.

Li, S.-C., Lindenberger, U., & Sikström, S. (2001). Aging cognition: from neuromodulation to representation. *Trends in Cognitive Sciences*, *5*(11), 479–486.

Libby, L. A., Hannula, D. E., & Ranganath, C. (2014). Medial temporal lobe coding of item and spatial information during relational binding in working memory. *Journal of Neuroscience*, *34*(43), 14233–14242.

Lindquist, M. A., & Wager, T. D. (2007). Validity and power in hemodynamic response modeling: A comparison study and a new approach. *Human Brain Mapping*, *28*(8), 764–784.

Loftus, E. F. (1991). The glitter of everyday memory…and the gold. *American Psychologist*, *46*(1), 16–18.

Loftus, E. F. (2013). 25 years of eyewitness science……finally pays off. *Perspectives on Psychological Science*, *8*(5), 556–557.

Luck, S. J., & Vogel, E. K. (1997). The capacity of visual working memory for features and conjunctions. *Nature*, *390*(6657), 279–281.

Luck, S. J., & Vogel, E. K. (2013). Visual working memory capacity: from psychophysics and neurobiology to individual differences. *Trends in Cognitive Sciences*, *17*(8), 391–400.

Luck, S. J., Girelli, M., McDermott, M. T., & Ford, M. A. (1997). Bridging the gap between monkey neurophysiology and human perception: An ambiguity resolution theory of visual selective attention. *Cognitive Psychology*, *33*(1), 64–87.

Lynn, S. K., Ibagon, C., Bui, E., Palitz, S. A., Simon, N. M., & Barrett, L. F. (2016). Working memory capacity is associated with optimal adaptation of response bias to perceptual sensitivity in emotion perception. *Emotion*, *16*(2), 155–163.

Ma, W. J., Husain, M., & Bays, P. M. (2014). Changing concepts of working memory. *Nature Neuroscience*, *17*(3), 347–356.

Mackay, M. (2015). Lupus brain fog: A biologic perspective on cognitive impairment, depression, and fatigue in systemic lupus erythematosus. *Immunologic Research*, *63*(1), 26–37.

Mackey, W. E., & Curtis, C. E. (2017). Distinct contributions by frontal and parietal cortices support working memory. *Scientific Reports*, *7*(1), 6188.

Macmillan, N. A., & Creelman, C. D. (2005). Detection Theory: A User's Guide. London, UK: Lawrence Erlbaum Associates, Publishers.

Maki, P. M., & Henderson, V. W. (2016). Cognition and the menopause transition. *Menopause*, *23*(7), 803–805.

Manjón, J. V., Coupé, P., Martí-Bonmatí, L., Collins, D. L., & Robles, M. (2009). Adaptive non-local means denoising of MR images with spatially varying noise levels. *Journal of Magnetic Resonance Imaging*, *31*(1), 192–203.

Marr, D. (1971). Simple Memory: A Theory for Archicortex. *Philosophical Transactions of the Royal Society of London B: Biological Sciences*, *262*(841), 23–81.

Marr, D. (1982). The philosophy and the approach. In D. Marr (Ed.), *Vision: A computational investigation into the human representation and processing visual information* (pp. 8–38). Boston: MIT Press.

McClelland, J. L., McNaughton, B. L., & OReilly, R. C. (1995). Why there are complementary learning systems in the hippocampus and neocortex: Insights from the successes and failures of connectionist models of learning and memory. *Psychological Review*, *102*(3), 419–457.

McLaren, D. G., Ries, M. L., Xu, G., & Johnson, S. C. (2012). A generalized form of context-dependent psychophysiological interactions (gPPI): A comparison to standard approaches. *NeuroImage*, *61*(4), 1277–1286.

Meng, X. L., Rosenthal, R., & Rubin, D. B. (1992). Comparing correlated correlation coefficients. *Psychological Bulletin*, *111*(1), 172–175.

Migliorati, M., Salvador, M., Adolescent, E. S.-N., 2012. (2012). In the first person: A window into the experience of early psychosis and recovery. *Adolescent Psychiatry*, *2*, 146–152.

Miller, E. K., & Buschman, T. J. (2015). Working memory capacity: Limits on the bandwidth of cognition. *Daedalus*, *144*(1), 112–122.

Miller, E. K., & Cohen, J. D. (2001). An integrative theory of prefrontal cortex function. *Annual Review of Neuroscience*, *24*(1), 167–202.

Miller, G. A. (1956). The magical number seven plus or minus two: Some limits on our capacity for processing information. *Psychological Review*, *63*(2), 81–97.

Miyake, A., & Shah, P. (1999). Models of working memory. New York: Cambridge University Press.

Modinos, G., Mechelli, A., Ormel, J., Groenewold, N. A., Aleman, A., & McGuire, P. K. (2009). Schizotypy and brain structure: a voxel-based morphometry study. *Psychological Medicine*, *40*(09), 1423–1431.

Moss, F. (2004). Stochastic resonance and sensory information processing: a tutorial and review of application. *Clinical Neurophysiology*, *115*(2), 267–281.

Myers, N. E., Stokes, M. G., & Nobre, A. C. (2017). Prioritizing information during working memory: Beyond sustained internal attention. *Trends in Cognitive Sciences*, *21*(6), 449–461.

Myers, N. E., Stokes, M. G., Walther, L., & Nobre, A. C. (2014). Oscillatory brain state predicts variability in working memory. *Journal of Neuroscience*, *34*(23), 7735–7743.

Nee, D. E., & Brown, J. W. (2012). Dissociable frontal–striatal and frontal–parietal networks involved in updating hierarchical contexts in working memory. *Cerebral Cortex*, *23*(9), 2146–2158.

Nee, D. E., & Jonides, J. (2013a). Neural evidence for a 3-state model of visual short-term memory. *NeuroImage*, *74*, 1–11.

Nee, D. E., & Jonides, J. (2013b). Trisecting representational states in short-term memory. *Frontiers in Human Neuroscience*, *7*, 796.

Noack, H., Lövdén, M., & Lindenberger, U. (2012). Normal aging increases discriminal dispersion in visuospatial short-term memory. *Psychology and Aging*, *27*(3), 627–637.

Nosofsky, R. M., & Donkin, C. (2016). Response-time evidence for mixed memory states in a sequential-presentation change-detection task. *Cognitive Psychology*, *84*, 31–62.

Oberauer, K. (2002). Access to information in working memory: Exploring the focus of attention. *Journal of Experimental Psychology: Learning, Memory, and Cognition*, *28*(3), 411–421.

Oberauer, K., & Lin, H.-Y. (2017). An interference model of visual working memory. *Psychological Review*, *124*(1), 21–59.

Ocon, A. J. (2013). Caught in the thickness of brain fog: Exploring the cognitive symptoms of Chronic Fatigue Syndrome. *Frontiers in Physiology*, *4*, 63.

Olson, I. R., Moore, K. S., Stark, M., & Chatterjee, A. (2006). Visual working memory is impaired when the medial temporal lobe is damaged. *Journal of Cognitive Neuroscience*, *18*(7), 1087–1097.

Paivio, A., & Bleasdale, F. (1974). Visual short-term memory: A methodological caveat. *Canadian Journal of Psychology/Revue Canadienne De Psychologie*, *28*(1), 24–31.

Palmer, J. (1990). Attentional limits on the perception and memory of visual information. *Journal of Experimental Psychology: Human Perception and Performance*, *16*(2), 332–350.

Parker, B. A., Polk, D. M., Rabdiya, V., Meda, S. A., Anderson, K., Hawkins, K. A., et al. (2010). Changes in Memory Function and Neuronal Activation Associated with Atorvastatin Therapy. *Pharmacotherapy*, *30*(6), 625–625.

Parks, C. M., & Yonelinas, A. P. (2007). Moving beyond pure signal-detection models: Comment on Wixted (2007). *Psychological Review*, *114*(1), 188–201.

Peich, M.-C., Husain, M., & Bays, P. M. (2013). Age-related decline of precision and binding in visual working memory. *Psychology and Aging*, *28*(3), 729–743.

Pitt, M. A., & Myung, I. J. (2002). When a good fit can be bad. *Trends in Cognitive Sciences*, *6*(10), 421–425.

Poliakov, E., Stokes, M. G., Woolrich, M. W., Mantini, D., & Astle, D. E. (2014). Modulation of alpha power at encoding and retrieval tracks the precision of visual short-term memory. *Journal of Neurophysiology*, *112*(11), 2939–2945.

Poppenk, J., Evensmoen, H. R., Moscovitch, M., & Nadel, L. (2013). Long-axis specialization of the human hippocampus. *Trends in Cognitive Sciences*, *17*(5), 230–240.

Pratte, M. S., Park, Y. E., Rademaker, R. L., & Tong, F. (2017). Accounting for stimulus-specific variation in precision reveals a discrete capacity limit in visual working memory. *Journal of Experimental Psychology: Human Perception and Performance*, *43*(1), 6–17.

Preston, A. R., & Eichenbaum, H. (2013). Interplay of Hippocampus and Prefrontal Review Cortex in Memory. *Current Biology*, *23*(17), R764–R773.

Prinzmetal, W., Amiri, H., Allen, K., & Edwards, T. (1998). Phenomenology of attention: I. Color, location, orientation, and spatial frequency. *Journal of Experimental Psychology: Human Perception and Performance*, *24*(1), 261–282.

Raffone, A., & Wolters, G. (2001). A cortical mechanism for binding in visual working memory. *Journal of Cognitive Neuroscience*, *13*(6), 766–785.

Ranganath, C., & Blumenfeld, R. S. (2005). Doubts about double dissociations between short- and long-term memory. *Trends in Cognitive Sciences*, *9*(8), 374–380.

Reagh, Z. M., & Yassa, M. A. (2014). Object and spatial mnemonic interference differentially engage lateral and medial entorhinal cortex in humans. *Proceedings of the National Academy of Sciences of the United States of American*, *111*(40), E4264–E4273.

Reagh, Z. M., Murray, E. A., & Yassa, M. A. (2017). Repetition reveals ups and downs of hippocampal, thalamic, and neocortical engagement during mnemonic decisions. *Hippocampus*, *27*(2), 169–183.

Richter, F. R., Cooper, R. A., Bays, P. M., Simons, J. S., & Davachi, L. (2016). Distinct neural mechanisms underlie the success, precision, and vividness of episodic memory. *eLife*, *5*, e18260.

Ringach, D. L., Shapley, R. M., & Hawken, M. J. (2002). Orientation selectivity in macaque V1: diversity and laminar dependence. *Journal of Neuroscience*, *22*(13), 5639–5651.

Roberts, S., & Pashler, H. (2000). How persuasive is a good fit? A comment on theory testing. *Psychological Review*, *107*(2), 358–367.

Roberts, S., & Pashler, H. (2002). Reply to Rodgers and Rowe (2002). *Psychological Review*, *109*(3), 605–607.

Rodgers, J. L., & Rowe, D. C. (2002). Postscript: Theory development should not end (but always begins) with good empirical fits: Response to Roberts and Pashler's (2002) reply. *Psychological Review*, *109*(3), 603–604.

Roggeman, C., Klingberg, T., Feenstra, H. E. M., Compte, A., & Almeida, R. (2014). Trade-off between capacity and precision in visuospatial working memory. *Journal of Cognitive Neuroscience*, *26*(2), 211–222.

Rolls, E. T. (2013). The mechanisms for pattern completion and pattern separation in the hippocampus. *Frontiers in Systems Neuroscience*, *7*, 74.

Rolls, E. T. (2016). Pattern separation, completion, and categorisation in the hippocampus and neocortex. *Neurobiology of Learning and Memory*, *129*(C), 4–28.

Rose, N. S., LaRocque, J. J., Riggall, A. C., Gosseries, O., Starrett, M. J., Meyering, E. E., & Postle, B. R. (2016). Reactivation of latent working memories with transcranial magnetic stimulation. *Science*, *354*(6316), 1136–1139.

Rosenthal, R., & DiMatteo, M. R. (2001). Meta-analysis: Recent developments in quantitative methods for literature reviews. *Annual Review of Psychology*, *52*, 59–82.

Rosenthal, R., Rosnow, R. L., & Rubin, D. B. (2000). Contrasts and effect sizes in behavioral research: A correlational approach. New York: Cambridge University Press.

Ross, A. J., Medow, M. S., Rowe, P. C., & Stewart, J. M. (2013). What is brain fog? An evaluation of the symptom in postural tachycardia syndrome. *Clinical Autonomic Research*, *23*(6), 305–311.

Roux, F., & Uhlhaas, P. J. (2014). Working memory and neural oscillations: α-γ versus θ-γ codes for distinct WM information? *Trends in Cognitive Sciences*, *18*(1), 16–25.

Roux, F., Wibral, M., Mohr, H. M., Singer, W., & Uhlhaas, P. J. (2012). Gamma-Band Activity in Human Prefrontal Cortex Codes for the Number of Relevant Items Maintained in Working Memory. *Journal of Neuroscience*, *32*(36), 12411–12420.

Sarma, A., Masse, N. Y., Wang, X.-J., & Freedman, D. J. (2015). Task-specific versus generalized mnemonic representations in parietal and prefrontal cortices. *Nature Neuroscience*, *19*(1), 143–149.

Sathian, K., Deshpande, G., & Stilla, R. (2013). Neural changes with tactile learning reflect decision-level reweighting of perceptual readout. *Journal of Neuroscience*, *33*(12), 5387–5398.

Sauseng, P., Klimesch, W., Heise, K. F., Gruber, W. R., Holz, E., Karim, A. A., et al. (2009). Brain oscillatory substrates of visual short-term memory capacity. *Current Biology*, *19*(21), 1846–1852.

Schmeichel, B. J., Volokhov, R. N., & Demaree, H. A. (2008). Working memory capacity and the self-regulation of emotional expression and experience. *Journal of Personality and Social Psychology*, *95*(6), 1526–1540.

Scimeca, J. M., Kiyonaga, A., & D'Esposito, M. (2018). Reaffirming the sensory recruitment account of working memory. *Trends in Cognitive Sciences*, *22*(3), 190–192.

Scott, W. A. (1962). Cognitive complexity and cognitive flexibility. *Sociometry*, *25*(4), 405–414.

Scoville, W. B., & Milner, B. (1957). Loss of recent memory after bilateral hippocampal lesions. *Journal of Neurology, Neurosurgery, and Psychiatry*, *20*(1), 11–21.

Segal, S. K., Stark, S. M., Kattan, D., Stark, C. E., & Yassa, M. A. (2012). Norepinephrine-mediated emotional arousal facilitates subsequent pattern separation. *Neurobiology of Learning and Memory*, *97*(4), 465–469.

Serences, J. T., Ester, E. F., Vogel, E. K., & Awh, E. (2009). Stimulus-specific delay activity in human primary visual cortex. *Psychological Science*, *20*(2), 207–214.

Severa, W., Parekh, O., James, C. D., & Aimone, J. B. (2017). A combinatorial model for dentate gyrus sparse coding. *Neural Computation*, *29*(1), 94–117.

Shohamy, D., & Turk-Browne, N. B. (2013). Mechanisms for widespread hippocampal involvement in cognition. *Journal of Experimental Psychology: General*, *142*(4), 1159–1170.

Simons, J. S., & Spiers, H. J. (2003). Prefrontal and medial temporal lobe interactions in long-term memory. *Nature Reviews Neuroscience*, *4*(8), 637–648.

Spachtholz, P., Kuhbandner, C., & Pekrun, R. (2014). Negative affect improves the quality of memories: Trading capacity for precision in sensory and working memory. *Journal of Experimental Psychology: General*, *143*(4), 1450–1456.

Sprague, T. C., Ester, E. F., & Serences, J. T. (2014). Reconstructions of information in visual spatial working memory degrade with memory load. *Current Biology*, *24*(18), 2174–2180.

Sprague, T. C., Ester, E. F., & Serences, J. T. (2016). Restoring latent visual working memory representations in human cortex. *Neuron*, *91*(3), 694–707.

Squire, L. R. (1986). Mechanisms of memory. *Science*, *232*(4758), 1612–1619.

Squire, L. R. (2017). Memory for relations in the short term and the long term after medial temporal lobe damage. *Hippocampus*, *27*(5), 608–612.

Squire, L. R., & Dede, A. J. O. (2015). Conscious and unconscious memory systems. *Cold Spring Harbor Perspectives in Biology*, *7*(3), a021667–15.

Squire, L. R., & Zola-Morgan, S. (1991). The medial temporal lobe memory system. *Science*, *253*(5026), 1380–1386.

Squire, L. R., Wixted, J. T., & Clark, R. E. (2007). Recognition memory and the medial temporal lobe: A new perspective. *Nature Reviews Neuroscience*, *8*(11), 872–883.

Standing, L. (1973). Learning 10000 pictures. *Quarterly Journal of Experimental Psychology*, *25*(2), 207–222.

Stark, S. M., Yassa, M. A., Lacy, J. W., & Stark, C. E. L. (2013). A task to assess behavioral pattern separation (BPS) in humans: Data from healthy aging and mild cognitive impairment. *Neuropsychologia*, *51*(12), 2442–2449.

Stokes, M. G. (2015). "Activity-silent" working memory in prefrontal cortex: a dynamic coding framework. *Trends in Cognitive Sciences*, *19*(7), 394–405.

Strange, B. A., Witter, M. P., Lein, E. S., & Moser, E. I. (2014). Functional organization of the hippocampal longitudinal axis. *Nature Neuroscience*, *15*(10), 655–669.

Sullvan, E. V., & Sagar, H. J. (1991). Double dissociation of short-term and long-term memory for nonverbal material in parkinson's disease and global amnesia: A further analysis. *Brain*, *114*(2), 893–906.

Suzuki, M. (2005). Differential contributions of prefrontal and temporolimbic pathology to mechanisms of psychosis. *Brain*, *128*(9), 2109–2122.

Takashima, A., Petersson, K. M., Rutters, F., Tendolkar, I., Jensen, O., Zwarts, M. J., et al. (2006). Declarative memory consolidation in humans: A prospective functional magnetic resonance imaging study. *Proceedings of the National Academy of Sciences of the United States of American*, *103*(3), 756–761.

Theoharides, T. C. (2015). Brain "fog," inflammation and obesity: key aspects of neuropsychiatric disorders improved by luteolin. *Frontiers in Neuroscience*, *9*, 1–11.

Theoharides, T. C., Stewart, J. M., Panagiotidou, S., & Melamed, I. (2016). Mast cells, brain inflammation and autism. *European Journal of Pharmacology*, *778*, 96–102.

Theoharides, T. C., Tsilioni, I., Patel, A. B., & Doyle, R. (2016). Atopic diseases and inflammation of the brain in the pathogenesis of autism spectrum disorders. *Translational Psychiatry*, *6*, e844.

Todd, J. J., & Marois, R. (2004). Capacity limit of visual short-term memory in human posterior parietal cortex. *Nature*, *428*(6984), 751–754.

Tustison, N. J., & Avants, B. B. (2013). Explicit B-spline regularization in diffeomorphic image registration. *Frontiers in Neuroinformatics*, (7), 39.

Tustison, N. J., Avants, B. B., Cook, P. A., Yuanjie Zheng, Egan, A., Yushkevich, P. A., & Gee, J. C. (2010). N4ITK: Improved N3 bias correction. *IEEE Transactions on Medical Imaging*, *29*(6), 1310–1320.

Tustison, N. J., Cook, P. A., Klein, A., Song, G., Das, S. R., Duda, J. T., et al. (2014). Large-scale evaluation of ANTs and FreeSurfer cortical thickness measurements. *NeuroImage*, *99*(C), 166–179.

Underwood, B. J. (1957). Interference and forgetting. *Psychological Review*, *64*(1), 49–60.

van den Berg, R., Awh, E., & Ma, W. J. (2014). Factorial comparison of working memory models. *Psychological Review*, *121*(1), 124–149.

Veldsman, M., Mitchell, D. J., & Cusack, R. (2017). The neural basis of precise visual short-term memory for complex recognisable objects. *NeuroImage*, *159*, 131–145.

Verghese, P. (2001). Visual search and attention: A signal detection theory approach. *Neuron*, *31*(4), 523–535.

Vogel, E. K., & Machizawa, M. G. (2004). Neural activity predicts individual differences in visual working memory capacity. *Nature*, *428*(6984), 748–751.

Voytek, B., & Knight, R. T. (2010). Prefrontal cortex and basal ganglia contributions to visual working memory. *Proceedings of the National Academy of Sciences of the United States of America*, *107*(42), 18167–18172.

Walitt, B., Čeko, M., Khatiwada, M., Gracely, J. L., Rayhan, R., VanMeter, J. W., & Gracely, R. H. (2016). Characterizing "fibrofog": Subjective appraisal, objective performance, and task-related brain activity during a working memory task. *NeuroImage: Clinical*, *11*(C), 173–180.

Wang, H., Suh, J. W., Das, S. R., Pluta, J. B., Craige, C., & Yushkevich, P. A. (2015). Multi-atlas segmentation with joint label fusion. *IEEE Transactions on Pattern Analysis and Machine Intelligence*, *35*(3), 611–623.

Wee, N., Asplund, C. L., & Chee, M. W. L. (2013). Sleep deprivation accelerates delay-related loss of visual short-term memories without affecting precision. *Sleep*, *36*(6), 849–856.

Wilken, P., & Ma, W. J. (2004). A detection theory account of change detection. *Journal of Vision*, *4*(12), 1120–1135.

Wimmer, K., Nykamp, D. Q., Constantinidis, C., & Compte, A. (2014). Bump attractor dynamics in prefrontal cortex explains behavioral precision in spatial working memory. *Nature Neuroscience*, *17*(3), 431–439.

Wixted, J. T. (2007). Dual-process theory and signal-detection theory of recognition memory. *Psychological Review*, *114*(1), 152–176.

Xie, W., & Zhang, W. (2016). Negative emotion boosts quality of visual working memory representation. *Emotion*, *16*(5), 760–774.

Xie, W., & Zhang, W. (2017a). Dissociations of the number and precision of visual short-term memory representations in change detection. *Memory & Cognition*, *45*(8), 1423–1437.

Xie, W., & Zhang, W. (2017b). Negative emotion enhances mnemonic precision and subjective feelings of remembering in visual long-term memory. *Cognition*, *166*, 73–83.

Xie, W., & Zhang, W. (2018). Mood-dependent retrieval in visual long-term memory: dissociable effects on retrieval probability and mnemonic precision. *Cognition and Emotion*, *32*(4), 674–690.

Xie, W., Cappiello, M., Park, H.-B., Deldin, P., Chan, R. C. K., & Zhang, W. (2018). Schizotypy is associated with reduced mnemonic precision in visual working memory. *Schizophrenia Research*, *193*, 91–97.

Xie, W., Li, H., Ying, X., Zhu, S., Fu, R., Zou, Y., & Cui, Y. (2017). Affective bias in visual working memory is associated with capacity. *Cognition and Emotion*, *31*(7), 1345–1360.

Xu, Y., & Chun, M. M. (2005). Dissociable neural mechanisms supporting visual short-term memory for objects. *Nature*, *440*(7080), 91–95.

Yassa, M. A., & Stark, C. E. L. (2011). Pattern separation in the hippocampus. *Trends in Neurosciences*, *34*(10), 515–525.

Yassa, M. A., Stark, S. M., Bakker, A., Albert, M. S., Gallagher, M., & Stark, C. E. L. (2010). High-resolution structural and functional MRI of hippocampal CA3 and dentate gyrus in patients with amnestic Mild Cognitive Impairment. *NeuroImage*, *51*(3), 1242–1252.

Yelland, G. W. (2017). Gluten-induced cognitive impairment ("brain fog") in coeliac disease. *Journal of Gastroenterology and Hepatology*, *32*(S1), 90–93.

Yonelinas, A. P. (2002). The nature of recollection and familiarity: A review of 30 years of research. *Journal of Memory and Language*, *46*(3), 441–517.

Yonelinas, A. P. (2013). The hippocampus supports high-resolution binding in the service of perception, working memory and long-term memory. *Behavioural Brain Research*, *254*, 34–44.

Yonelinas, A. P., & Parks, C. M. (2007). Receiver operating characteristics (ROCs) in recognition memory: A review. *Psychological Bulletin*, *133*(5), 800–832.

Yonelinas, A. P., Aly, M., Wang, W.-C., & Koen, J. D. (2010). Recollection and familiarity: Examining controversial assumptions and new directions. *Hippocampus*, *20*(11), 1178–1194.

Yushkevich, P. A., Wang, H., Pluta, J., Das, S. R., Craige, C., Avants, B. B., et al. (2010). Nearly automatic segmentation of hippocampal subfields in in vivo focal T2-weighted MRI. *NeuroImage*, *53*(4), 1208–1224.

Zhang, W. (2007). *Resolution and capacity limitations in visual working memory: A new approach (Doctoral dissertation)*. Retrieved from ProQuest Dissertations & Theses. (Publication No. 3266021).

Zhang, W., & Luck, S. J. (2008). Discrete fixed-resolution representations in visual working memory. *Nature*, *453*(7192), 233–235.

Zhang, W., & Luck, S. J. (2009). Sudden death and gradual decay in visual working memory. *Psychological Science*, *20*(4), 423–428.

Zhang, W., & Luck, S. J. (2011). The number and quality of representations in working memory. *Psychological Science*, *22*(11), 1434–1441.

Zhang, W., & Yonelinas, A. P. (2012). The influence of medial temporal lobe damage on capacity and precision in visual working memory. Presented at the Annual Meeting of the Cognitive Neuroscience Society, Chicago, IL.